1972-06

Analysis of a heated jet in a stream

Champagne, Gerald Edward

http://hdl.handle.net/10945/15978

ANALYSIS OF A HEATED JET IN A STREAM

Gerald Edward Champagne

NAVAL POSTGRADUATE SCHOOL
Monterey, California

THESIS

ANALYSIS OF A HEATED JET IN A STREAM

by

Gerald Edward Champagne

Thesis Advisor: M. Kelleher

June 1972

Analysis of a Heated Jet in a Stream

by

Gerald Edward Champagne
Ensign, United States Navy
B.S., Tulane University, 1971

Submitted in partial fulfillment of the
requirements for the degree of

MASTER OF SCIENCE IN MECHANICAL ENGINEERING

from the

NAVAL POSTGRADUATE SCHOOL
June 1972

ABSTRACT

A plane, heated jet of a constant property fluid exiting into a plane, straight channel of the same fluid is analyzed. The effect of buoyancy on the velocity and temperature fields is investigated. Two jet orientations are considered; a transverse jet, which enters the stream perpendicular to the main flow, and a longitudinal jet, which enters the stream parallel to the main flow.

Solutions for the temperature and velocity fields for low Reynolds number flow are obtained using a finite difference scheme. Results are presented for three different values of the buoyant force, holding other variables constant. For an isothermal jet, results for the velocity field are presented at a higher Reynolds number.

TABLE OF CONTENTS

I. INTRODUCTION ---------------------------------- 8

II. ANALYSIS -- 12

- A. COORDINATE SYSTEM -------------------------- 12
- B. GOVERNING EQUATIONS ------------------------ 12
- C. BOUNDARY CONDITIONS ------------------------ 16

III. METHOD OF SOLUTION ---------------------------- 25

- A. GOVERNING EQUATIONS ------------------------ 25
- B. BOUNDARY CONDITIONS IN FINITE DIFFERENCE FORM ---------------------------- 29
- C. NUMERICAL SOLUTION SCHEME ----------------- 38

IV. RESULTS --- 47

- A. PRESENTATION OF RESULTS -------------------- 47
- B. DISCUSSION OF RESULTS --------------------- 54

V. DISCUSSION -------------------------------------- 69

- A. CONVERGENCE OF LINEAR SOLUTION FOR STREAM FUNCTION --------------------------- 69
- B. NUMERICAL STABILITY OF ITERATIVE SCHEME --- 73
- C. CONCLUSIONS -------------------------------- 74
- D. RECOMMENDATIONS --------------------------- 76

APPENDIX A - COMPUTER PROGRAM USED TO DEVELOP FINITE DIFFERENCE OPERATORS ------------ 79

APPENDIX B - COMPUTER PROGRAM USED IN NUMERICAL SOLUTION ------------------------------- 84

LIST OF REFERENCES --------------------------------- 94

INITIAL DISTRIBUTION LIST --------------------------- 96

FORM DD 1473 -- 97

NOMENCLATURE

List of Symbols

a	Thermal diffusivity
c	Specific heat
C_i	Coefficients of interpolating polynomial
D	Channel depth
D_j	Width of jet
D_j^*	Non-dimensional width of jet
F	Unknown general function
g	Acceleration of gravity
Gr	Grashof number based on channel depth
h	Coefficient of heat transfer
H	Grid spacing in vertical direction
$J\ (A,B)$	Jacobian operator
k	Thermal conductivity
K_i	Coefficients of finite difference approximation
M	Square matrix
p	Pressure
$P\ (x,y)$	Interpolating polynomial
Pr	Prandtl number
q	Heat flux
Re	Reynolds number based on channel depth
T	Temperature
T_o	Undisturbed stream temperature
u	Velocity in horizontal direction

U	Non-dimensional velocity in horizontal direction
U_j	Non-dimensional jet velocity
U_o	Average undisturbed stream velocity
U_s	Surface velocity
v	Velocity in vertical direction
V	Non-dimensional velocity in vertical direction
$V_i\ (x,y)$	Variable terms of interpolating polynomial
x	Space coordinate in horizontal direction
X	Non-dimensional space coordinate in horizontal direction
y	Space coordinate in vertical direction
Y	Non-dimensional space coordinate in vertical direction
α	Ratio of grid spacing in horizontal direction to spacing in vertical direction
β	Coefficient of thermal expansion
θ	Non-dimensional temperature
θ^{ℓ}	Solution for θ at ℓ^{th} iteration
μ	Absolute viscosity
ν	Kinematic viscosity
ρ	Density
ψ	Stream function
ψ^*	Non-dimensional stream function
$\psi^{*\ell}$	Solution for ψ^* at ℓ^{th} iteration
∇^2	Harmonic operator
∇^4	Biharmonic operator
$< >$	Row vector
$\{ \}$	Column vector
$[ ]$	Square matrix
$\mathcal{O}$	Order of

List of Subscripts

a	Ambient
D	Downstream boundary
i	Incoming stream
j	Jet
jL	Lower edge of jet
jU	Upper edge of jet
L	Longitudinal jet
max	Maximum
s	Surface
T	Transverse jet
u	Upstream boundary

ACKNOWLEDGEMENTS

The author wishes to acknowledge the assistance, guidance, and encouragement given by his advisor, Professor Matthew Kelleher. The author also wishes to thank his wife, Diane, for her patience and support throughout this work, and to thank Professor Gilles Cantin for his assistance in the numerical work.

The Naval Postgraduate School Computer Center provided facilities for the computer work.

I. INTRODUCTION

Every commercial power generation plant releases some waste heat to the environment. Water from a nearby stream, lake, ocean is normally used as a reservoir for this rejected heat. As the demand for power increases, more and more heat will be discharged into these bodies of water. The advent of nuclear power plants, which have a lower thermal efficiency than conventional fossil-fueled plants will tend to increase the amount of waste heat per unit power output. With the emergence of these trends, concern about the effect of these thermal discharges has begun to grow.

The utilization of a body of water for cooling purposes is normally carried out by diverting a certain mass flow from the body of water, passing it through a heat exchanger, and returning it at an increased temperature. Hence, the temperature of the body of water, at least in the local sense, is increased.

From the biological viewpoint, there is no doubt that raising the temperature of water can be harmful to some forms of aquatic life. For example, for some fish a seasonal temperature rise of as little as 2°C can be fatal. Aside from such obvious damage, raising the temperature of water decreases its capability to retain dissolved oxygen, increases the metabolic rate of fish, and affects their reproductive habits and ability to resist disease. In addition, an increase in environmental temperature is beneficial to some

[illegible]

[illegible]

[illegible]

potentially harmful forms of plant life and bacteria [1]. Although the immediate effect of such changes may not be obvious, the normal equilibrium of the ecological system has been disturbed, and the possibility of long range damage does exist.

In order to ensure that temperature disturbances are within safe limits, the precise nature of the temperature disturbance must be known. The quantitative value of the increase in temperature above the undisturbed temperature of the given body of water as a function of position and time would be of significant value in analyzing the effect of a thermal discharge. Several studies related to this problem have been carried out.

The overall effect of a thermal discharge on a given body of water is one method of approaching the problem. A method for predicting the equilibrium temperature of a cooling lake was described by Sefchovich [2]. A study relating plant parameters to the average upstream temperature in a stream or river was developed by Nahavandi and Campisi [3].

An experimental investigation of the temperature profiles in the vicinity of a cooling plant located on Yankee River was presented by Merriam [4]. Approximate analytical models were compared with various experimental temperature profiles downstream of power plants situated on rivers by Polk, Benedict, and Lahey [5].

A possible model of a thermal discharge is a heated jet exiting into a given environment. For the case of thermal

discharge into a lake or ocean this model takes the form of a heated jet exiting into a quiescent fluid. An analytical solution for the two dimensional temperature and velocity profiles for the case of a heated, vertical , laminar jet exiting into an infinite environment was developed by Brand and Lahey [6]. Additional work on a heated jet exiting into a quiescent fluid is now being conducted at Oregon State University [7].

The case of a heated discharge into a stream or river may be modeled by a heated jet exiting into a moving stream. An experimental investigation of a buoyant, turbulent, circular air jet exiting into a cross wind was conducted by Ramsey and Goldstein [8]. An analytical study of the surface spread of a submerged, buoyant incompressible jet was made by Tulin and Schwartz [9].

The problem undertaken in this study was that of a heated jet in a stream. This particular problem can be approached in several ways. The general problem is a transient problem in which the temperature and velocity fields vary in three dimensions. Factors which must be considered are diurnal temperature and heat flux variations, tidal effects, seasonal temperature and flow variations, atmospheric conditions, stream meander path, bottom contour variations, fluid property variations, the possible turbulent nature of the effluent, and temperature stratification effects. Because of the complexity of this problem, several simplifications were made.

The transient conditions were assumed to be "slow" compared to the response time of the stream. Therefore, at any instant in time the stream could be considered to be at a quasi-equilibrium state. The time dependent terms were therefore not considered. The fluid properties were assumed to be constant, for simplification, and the axis of the river was assumed to be straight.

It was decided to attempt to isolate the effects of buoyancy on the temperature and flow patterns. Also, to put the problem in a more tractable form, it was decided to consider variations in two dimensions only. Assuming that one of the dimensions would be the downstream dimension, there are two possible choices: a plane parallel to the river surface or a vertical plane passing through the axis of the river. Since the buoyancy forces act in the vertical plane, the vertical plane was chosen. In order to isolate buoyant effects, the bottom of the channel was assumed to be straight and parallel to the river surface. Also, for simplification, the river and the jet were assumed to be laminar in nature. The desired solutions were the temperature and velocity profiles as a function of position and significant non-dimensional parameters.

II. ANALYSIS

A. COORDINATE SYSTEM

The problem under consideration in this work is flow in a channel into which a known quantity of fluid is injected. The injected fluid is at a higher temperature than the fluid in the channel. Since it is desired to study the effects of buoyancy, variations in the vertical plane only are considered. The axis of the river is assumed to be straight. Rectangular cartesian coordinates are used, as shown in Figure 1.

Two different orientations of the injected mass with respect to the main flow are considered. The longitudinal jet is injected parallel to the direction of main flow. The transverse jet is injected perpendicular to the direction of main flow. For the longitudinal jet, the origin of the coordinate system is located at the channel bottom, immediately below the jet location. For the transverse jet, the origin of the coordinate system is located far enough upstream of the jet so that the incoming temperature and velocity profiles are not disturbed (see Figure 1).

B. GOVERNING EQUATIONS

Applying the Boussinesq approximation, which assumes that all density variations other than those giving rise to the buoyant forces may be neglected, and neglecting viscous dissipation, the steady two dimensional forms of the continuity, Navier-Stokes, and energy equations are:

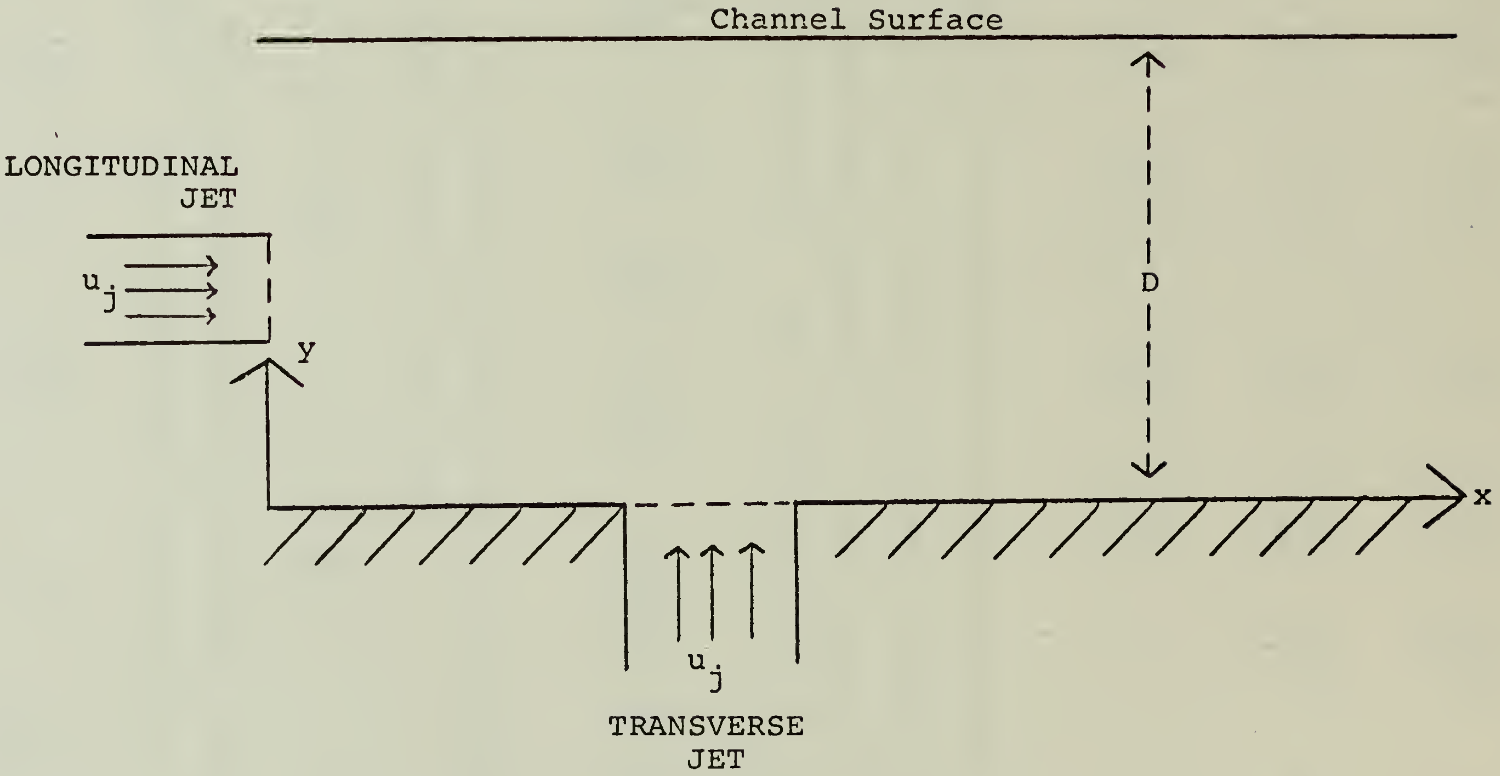

Figure 1 - Coordinate System

$$\frac{\partial u}{\partial x} + \frac{\partial v}{\partial y} = 0 \qquad (1)$$

$$\rho[u \frac{\partial u}{\partial x} + v \frac{\partial u}{\partial y}] = - \frac{\partial p}{\partial x} + \mu[\frac{\partial^2 u}{\partial x^2} + \frac{\partial^2 u}{\partial y^2}] \qquad (2)$$

$$\rho[u \frac{\partial v}{\partial x} + v \frac{\partial v}{\partial y}] = - \frac{\partial p}{\partial y} + \mu[\frac{\partial 2v}{\partial x2} + \frac{\partial^2 v}{\partial y^2}] + \rho g \beta[T-T_o] \qquad (3)$$

$$\rho c[u \frac{\partial T}{\partial x} + v \frac{\partial T}{\partial y}] = k[\frac{\partial^2 T}{\partial x^2} + \frac{\partial^2 T}{\partial y^2}] \qquad (4)$$

where T_o is the incoming stream temperature.

By cross-differentiating with respect to x and y, and by subtracting equation (3) from equation (2), the pressure p is eliminated. The resulting equation is:

$$u \frac{\partial^2 u}{\partial x \partial y} + v \frac{\partial^2 u}{\partial y^2} - u \frac{\partial^2 v}{\partial x^2} - v \frac{\partial^2 v}{\partial x \partial y} = \nu[\frac{\partial^3 u}{\partial x^2 \partial y} + \frac{\partial^3 u}{\partial y^3} - \frac{\partial^3 v}{\partial x^3} - \frac{\partial^3 v}{\partial x \partial y^2}] - g\beta \frac{\partial T}{\partial x} \qquad (5)$$

The continuity equation may be eliminated by defining a stream function ψ, such that

$$u = \frac{\partial \psi}{\partial y} \quad , \quad v = - \frac{\partial \psi}{\partial x}$$

Only two unknown quantities remain to be determined, ψ and T. The two remaining equations are

$$\frac{\partial \psi}{\partial y} [\frac{\partial \nabla^2 \psi}{\partial x}] - \frac{\partial \psi}{\partial x} [\frac{\partial \nabla^2 \psi}{\partial y}] = \nu \nabla^4 \psi - g\beta \frac{\partial T}{\partial x} \qquad (6)$$

$$\frac{\partial \psi}{\partial y} \frac{\partial T}{\partial x} - \frac{\partial \psi}{\partial x} \frac{\partial T}{\partial y} = a \nabla^2 T \qquad (7)$$

Equation (6) is the momentum equation expressed as the transport of vorticity, where the vorticity is defined as $\nabla^2\psi$.

The equations will be non-dimensionalized by introducing the following variables:

$$U = \frac{u}{U_o}$$

$$V = \frac{v}{V_o}$$

$$X = \frac{x}{D}$$

$$Y = \frac{y}{D}$$

$$\theta = \frac{T - T_o}{T_j - T_o}$$

$$\psi^* = \frac{\psi}{U_oD}$$

where U_o is the average undisturbed velocity, D is the channel depth, and T_j is the jet temperature.

By substituting these into equations (6) and (7),

$$\frac{\partial\psi^*}{\partial Y}\left[\frac{\partial\nabla^2\psi^*}{\partial X}\right] - \frac{\partial\psi^*}{\partial X}\left[\frac{\partial\nabla^2\psi^*}{\partial Y}\right] = \frac{1}{Re}\nabla^4\psi^* - \frac{Gr}{Re^2}\frac{\partial\theta}{\partial X} \qquad (8)$$

$$\frac{\partial\psi^*}{\partial Y}\frac{\partial\theta}{\partial X} - \frac{\partial\psi^*}{\partial X}\frac{\partial\theta}{\partial Y} = \frac{1}{RePr}\nabla^2\theta \qquad (9)$$

where Re is the Reynolds number based on the channel depth, Pr is the Prandtl number of the fluid, and Gr is the Grashof number based on the channel depth and the temperature difference between the jet temperature and the incoming stream temperature.

C. BOUNDARY CONDITIONS

Examination of the governing equations reveals that twelve boundary conditions are necessary to completely specify the problem. The necessary conditions are four conditions for ψ on x, four for ψ on y, two for T on x and two for T on y. These conditions will be specified on the channel bottom, the river surface, upstream and far downstream of the jet. The boundary conditions for ψ are first expressed in terms of velocity, and then related to the stream function from the definition of ψ, i.e., $\frac{\partial \psi}{\partial y} = u$, $\frac{\partial \psi}{\partial x} = -v$.

At the upstream boundary, the undisturbed incoming horizontal velocity profile is assumed to be a 20% truncated parabola, which is a common assumption in stream flow [10]. A 20% truncated parabolic flow profile has the maximum velocity located two tenths of the total depth below the free surface (see Figure 2). For the longitudinal jet, this profile is modified by assuming that the stream velocity is equal to the jet velocity across the jet width (see Figure 3). For the transverse jet, the upstream boundary is located far enough upstream so that the velocity profile is equal to the undisturbed velocity profile. The

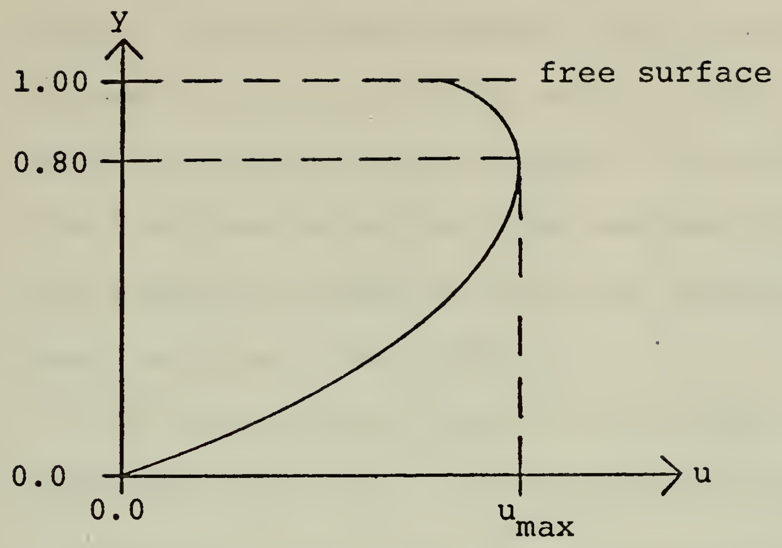

Figure 2 - 20% truncated parabolic velocity profile.

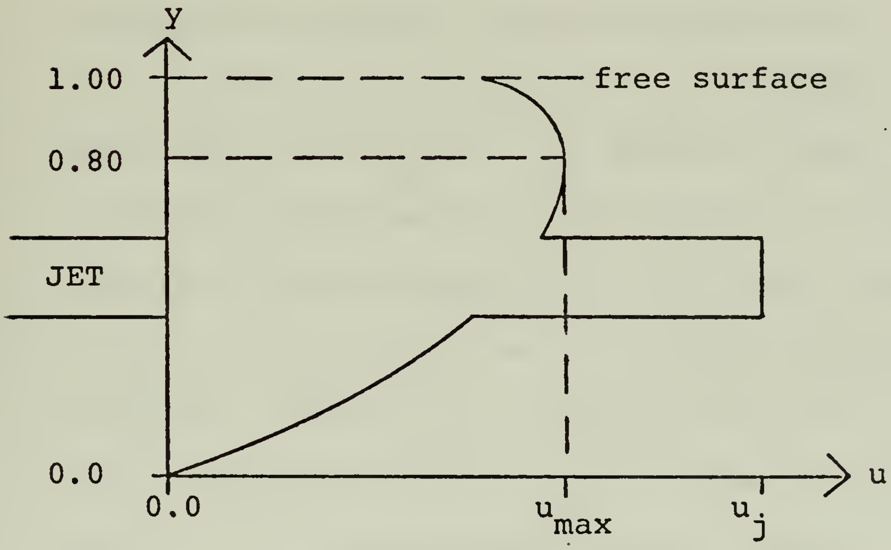

Figure 3 - Velocity profile at upstream boundary for longitudinal jet.

vertical component of the stream velocity is assumed to be zero. For the longitudinal jet, the stream temperature is assumed to be equal to T_o except across the jet width, where the temperature is equal to the jet temperature, T_j. For the transverse jet, the upstream boundary is located far enough upstream so that the incoming temperature profile is also undisturbed.

On the channel bottom, the no slip boundary condition requires that $u = 0$. The vertical component of velocity is also equal to zero, except at the transverse jet. In that case, v is equal to zero along the river bottom except across the jet width, where v is equal to the jet velocity. The river bottom is assumed to be adiabatic, yielding a temperature gradient boundary condition.

On the channel surface, it is assumed that there are no waves; i.e., $v = 0$. By assuming that the pressure is constant, and that the river surface is level, the application of the Bernoulli equation along the channel surface leads to the result that the surface velocity U_s is constant. Since U_s is constant, and the value of U_s at the upstream boundary is known, the surface velocity is equal to the undisturbed surface velocity. At the surface, the conductive, convective, and evaporative nodes of heat transfer to the atmosphere are lumped into an overall heat transfer coefficient. It is assumed that radiative heat fluxes can be modeled by a known constant heat flux q.

A simple heat balance shows that the heat conducted into the surface plus the radiative heat flux into the surface equals the heat convected out.

The velocity profile at the downstream boundary is assumed to be parabolic in form such that the total mass flow is equal to the undisturbed mass flow plus the mass flow of the jet. The vertical component of velocity is assumed to be equal to zero. It is also assumed that all heat added by the jet is convected out of the channel through the surface. Hence, the temperature profile returns to its original constant value T_o. The downstream boundary is situated far enough downstream so that the above conditions are met within a given tolerance.

The mathematical forms of these conditions are:

$$x=0 \qquad u_L = \frac{\partial \psi_L}{\partial y} = u_i(y) = \frac{U_s}{3}\left[8\left(\frac{y}{D}\right) - 5\left(\frac{y}{D}\right)^2\right] \qquad 0 \leq y < y_{jL}$$

$$= u_j \qquad y_{jL} < y < y_{jU}$$

$$= u_i(y) \qquad y_{ju} < y \leq D$$

$$u_T = \frac{\partial \psi_T}{\partial y} = u_i(y)$$

$$v = -\frac{\partial \psi}{\partial x} = 0$$

$$T_L = T_o \qquad 0 \leq y < y_{jL}$$

$$= T_j \qquad y_{jL} < y < y_{jU}$$

$$= T_o \qquad y_{jU} < y < D$$

$$T_T = T_o$$

$$y=0 \qquad u = \frac{\partial \psi}{\partial y} = 0$$

$$v_L = - \frac{\partial \psi}{\partial x} = 0$$

$$v_T = - \frac{\partial \psi}{\partial x} = 0 \qquad 0 \leq x < x_{jL}$$

$$= u_j \qquad x_{jL} < x < x_{jL}$$

$$= 0 \qquad x_{ju} < x$$

$$\frac{\partial T_L}{\partial y} = 0$$

$$\frac{\partial T_T}{\partial y} = 0 \qquad 0 \leq x < x_{jL}$$

$$T_T = T_j \qquad x_{jL} < x < x_{jU}$$

$$\frac{\partial T_T}{\partial y} = 0 \qquad x_{ju} < x$$

$$y = D \qquad u = \frac{\partial \psi}{\partial y} = U_s$$

$$v = - \frac{\partial \psi}{\partial x} = 0$$

$$q - k \frac{\partial T}{\partial y} = h(T-T_a)$$

$$x \to \infty \qquad u = \frac{\partial \psi}{\partial y} = u_D(y)$$

$$v = - \frac{\partial \psi}{\partial x} = 0$$

$$T = T_o$$

where the L subscript refers to the longitudinal jet, the T subscript refers to the transverse jet, the i subscript refers to the incoming velocity profile, the D subscript refers to the velocity profile at the downstream boundary, y_{jL} is the y-location of the lower edge of the jet, y_{jU} is the y-location of the upper edge of the jet, x_{jL} and x_{jU} are defined similarly for the x-location of the jet, and T_a is the ambient air temperature.

Since the problem is cast in terms of the stream function ψ, it is desired to reduce the boundary conditions to a more convenient form. At the undisturbed upstream boundary, the 20% truncated parabola gives the following form for the velocity profile.

$$u = \frac{\partial\psi}{\partial y} = \frac{U_s}{3}\left[8\,\frac{y}{D} - 5\left(\frac{y}{D}\right)^2\right]$$

Integrating from 0 to D, it was found that the average velocity U_o is given by

$$U_o = \frac{7}{9}\,U_s$$

Now, integrating u (y) from zero to y, assuming $\psi(x,0) = 0$

$$\psi_u = \frac{U_o D}{7}\left[12\left(\frac{y}{D}\right)^2 - 5\left(\frac{y}{D}\right)^3\right]$$

This is the upstream boundary condition for ψ for the transverse jet. For the longitudinal jet, if it is assumed

that the jet diameter is small with respect to the river depth, the expression for ψ becomes:

$$
\begin{aligned}
\psi &= \psi_u(y) && 0 \leq y < y_{jL} \\
&= \psi_u(y) + u_j D_j \left(\frac{y - y_{jL}}{D_j}\right) && y_{jL} < y < y_{jU} \\
&= \psi_u(y) && y_{jU} < y \leq D
\end{aligned}
$$

where D_j is the jet width, y_{jL} is the location of the lower edge of the jet, and y_{jU} is the location of the upper edge of the jet.

For the longitudinal jet, the boundary condition at the channel bottom may be satisfied by assuming ψ is constant. Hence, ψ is chosen to be zero on the channel bottom for this case.

For the transverse jet, the boundary condition for v may be integrated, giving

$$
\begin{aligned}
\psi_T &= 0 && \text{for} \quad x < x_{jL} \\
\psi_T &= -u_j D_j \left(\frac{x - x_{jL}}{D_j}\right) && x_{jL} < x < x_{jU} \\
\psi_T &= -u_j D_j && x > x_{jU}
\end{aligned}
$$

The boundary condition for v at the surface may also be satisfied by choosing ψ = constant. The value of the constant is equal to the value of ψ at the surface as given by the upstream boundary condition.

The downstream boundary condition for ψ may be found by integrating the downstream velocity profile, and evaluating constants from the surface and bottom values for ψ.

After performing the indicated operations, and nondimensionalizing, the final form of the boundary conditions becomes

$$X=0 \qquad \psi_T^*(Y) = \psi_u^*(Y) = \frac{1}{7}\,(12Y^2 - 5Y^3)$$

$$\psi_L^*(Y) = \begin{cases} \psi_U^*(Y) & 0 \le Y < Y_{jL} \\ \psi_U^*(Y_{jL}) + U_j D_j^*\left(\dfrac{Y - Y_{jL}}{D_j^*}\right) & Y_{jL} < Y < Y_{jU} \\ \psi_U^*(Y) + U_j D_j^* & Y_{jU} < Y < 1 \end{cases}$$

$$\frac{\partial \psi^*}{\partial X} = 0$$

$$\theta_T = 0$$

$$\theta_L = \begin{cases} 0 & 0 \le Y \le Y_{jL} \\ 1 & Y_{jL} \le Y \le Y_{jU} \\ 0 & Y_{jU} < Y < 1 \end{cases}$$

$$Y=0 \qquad \psi_L^* = 0$$

$$\psi_T^* = \begin{cases} 0 & 0 \le X < X_{jL} \\ -U_j D_j^*\left(\dfrac{X - X_{jL}}{D_j}\right) & X_{jL} < X < X_{jU} \\ -U_j D_j^* & X_{jU} < X \end{cases}$$

$$\frac{\partial \psi^*}{\partial Y} = 0$$

$$\frac{\partial \theta_L}{\partial Y} = 0$$

$$\frac{\partial \theta_T}{\partial Y} = 0 \qquad 0 \leq X < X_{jL}$$

$$\theta_T = 1 \qquad X_{jL} < X < X_{jU}$$

$$\frac{\partial \theta_T}{\partial Y} = 0 \qquad X_{jU} < X$$

$$Y=1 \qquad \frac{\partial \psi^*}{\partial Y} = \frac{9}{7}$$

$$\psi_T^* = 1$$

$$\psi_L^* = 1 + U_j D_j^*$$

$$\frac{\partial \theta}{\partial Y} - \frac{hD}{K}\theta = \frac{hD}{K}(Q - \theta_A)$$

$$X \to \infty \qquad \psi_L^* = \psi_D^*(Y) = \left(\frac{12}{7} + 3U_j D_j^*\right)Y^2 + \left(2U_j D_j^* - \frac{5}{7}\right)Y^3$$

$$\psi_T^* = \psi_D^*(Y) - U_j D_j^*$$

$$\frac{\partial \psi^*}{\partial X} = 0$$

$$\theta = 0$$

where the L and T subscripts have the same meaning as defined previously.

III. METHOD OF SOLUTION

A. GOVERNING EQUATIONS

The governing equations for the problem under consideration are:

$$\frac{\partial\psi^*}{\partial Y}\left(\frac{\partial\nabla^2\psi^*}{\partial X}\right) - \frac{\partial\psi^*}{\partial X}\left(\frac{\partial\nabla^2\psi^*}{\partial Y}\right) = \frac{1}{Re}\nabla^4\psi^* - \frac{Gr}{Re^2}\frac{\partial\theta}{\partial X} \tag{10}$$

$$\frac{\partial\psi^*}{\partial Y}\frac{\partial\theta}{\partial X} - \frac{\partial\psi^*}{\partial X}\frac{\partial\theta}{\partial Y} = \frac{1}{RePr}\nabla^2\theta \tag{11}$$

In order to solve this problem using a finite difference method, a finite difference operator for each differential operator in the governing equation is required. The method used to determine these operators is basically the same as that used by Dias [11]. The operators developed in this study, however, are applicable to rectangular grid networks as well as to square grid networks.

The procedure for determining the finite difference operators is to first define an interpolating polynomial P (x, y) having n undetermined coefficients. This polynomial can be used as an approximate to any general function F. (F can be interpreted as a stream function, for example.) By requiring that P (x, y) be equal to F at each of n points, n equations involving the n undetermined coefficients are generated. Hence, the coefficients of P (x, y) can be determined in terms of the value of F at each node.

By applying the desired differential operator to P (x, y), an approximation for the operator in terms of the value of F at each node is obtained.

To develop the biharmonic operator, a polynomial must be chosen such that the fourth partial derivatives with respect to both x and y are non-zero. The grid network through which P (x, y) is to be passed is shown in Figure 4. Since there are 25 points in this grid, 25 unknown coefficients are required in the polynomial P (x, y). Hence, an appropriate choice for P (x, y) is

$$\begin{aligned} P(x,y) = {} & C_1 y^4 x^4 + C_2 y^3 x^4 + C_3 y^2 x^4 + C_4 y x^4 + C_5 x^4 \\ & + C_6 y^4 x^3 + C_7 y^3 x^3 + C_8 y^2 x^3 + C_9 y x^3 + C_{10} x^3 \\ & + C_{11} y^4 x^2 + C_{12} y^3 x^2 + C_{13} y^2 x^2 + C_{14} y x^2 + C_{15} x^2 \\ & + C_{16} y^4 x + C_{17} y^3 x + C_{18} y^2 x + C_{19} y x + C_{20} x \\ & + C_{21} y^4 + C_{22} y^3 + C_{23} y^2 + C_{24} y + C_{25} \end{aligned} \tag{12}$$

This equation may be written in matrix form as:

$$P(x,y) = \langle V_i(x,y) \rangle \quad \{C_i\} \qquad i = 1,2,\ldots,25 \tag{13}$$

where V_i (x, y) is $x^p y^q$ corresponding to C_i in equation (12).

This polynomial is now required to pass through the value of F_j at each node j, where F_j is the value of the function F at node j. At each node j, the following relation is obtained:

$$P(x_j,y_j) = \langle V_i(x_j,y_j) \rangle \quad \{C_i\} = F_j \qquad i = 1,2,\ldots,25 \tag{14}$$

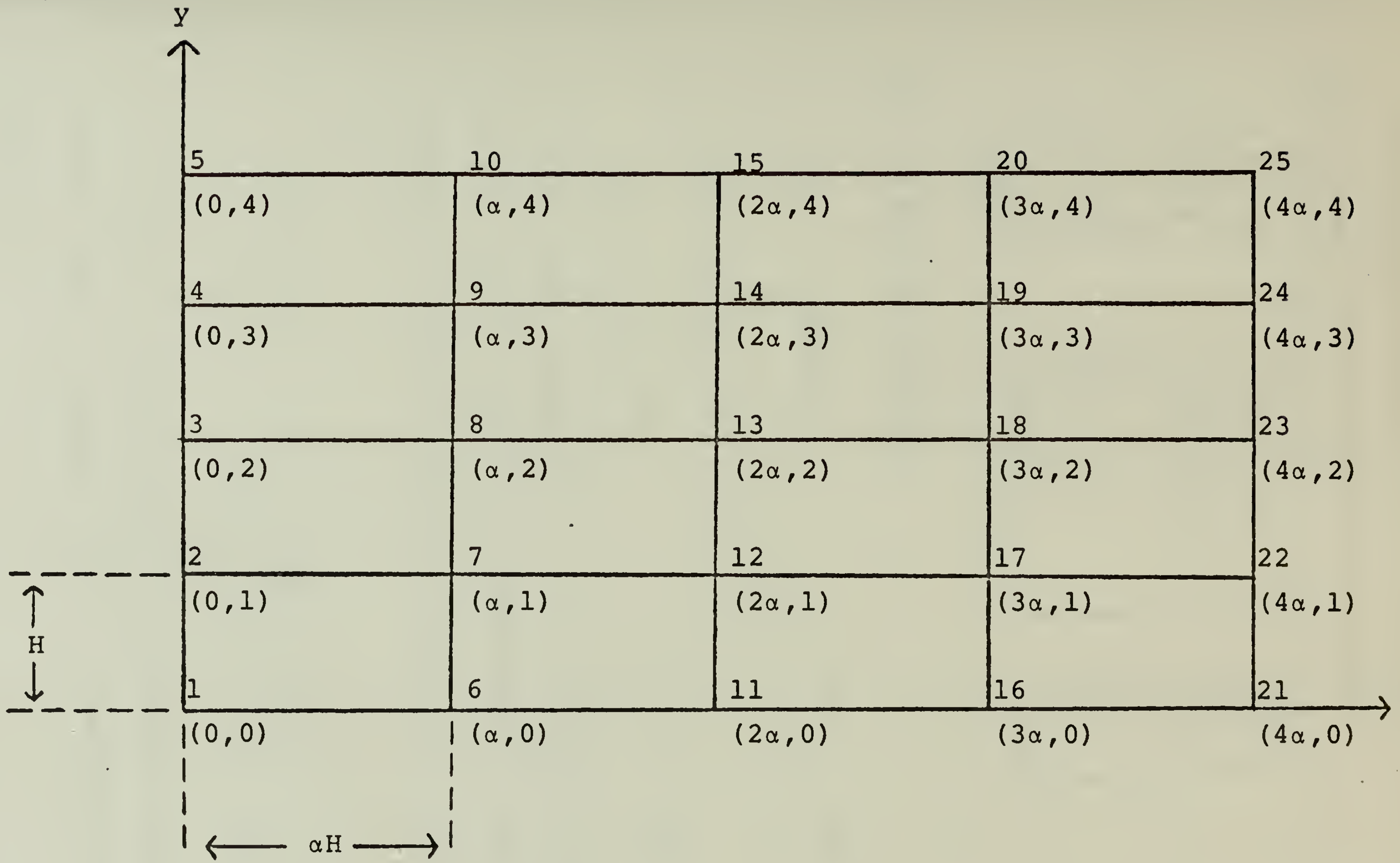

Figure 4 - 5 x 5 rectangular grid.

By applying this relation at each of the 25 grid points, the following set of equations results:

$$\begin{Bmatrix} F_1 \\ F_2 \\ \cdot \\ \cdot \\ \cdot \\ F_{25} \end{Bmatrix} = \begin{bmatrix} <V_i(x_1,y_1)> \\ <V_i(x_2\ y_2)> \\ \cdot \\ \cdot \\ \cdot \\ <V_i(x_{25},y_{25})> \end{bmatrix} \begin{Bmatrix} C_1 \\ C_2 \\ \cdot \\ \cdot \\ \cdot \\ C_{25} \end{Bmatrix} \qquad j = 1,2,\ldots,25 \qquad (15)$$

Or, in matrix notation:

$$\{F_j\} = [M]\{C_j\} \qquad j = 1,2,\ldots,25 \qquad (16)$$

Solving this matrix equation for C_j,

$$\{C_j\} = [M]^{-1}\{F_j\} \qquad j = 1,2,\ldots,25$$

The coefficients C_j of P (x, y) are now known, and P (x, y) can be used as an approximation for F. The biharmonic operator may now be applied to the polynomial P (x, y).

$$\begin{aligned} \nabla^4(P(x,y)) &= <\nabla^4\ (\ V_i(x,y)>\ \{C_i\}) \\ &= \nabla^4<(V_i(x,y))>\ \{C_i\} \qquad i = 1,2,\ldots,25 \end{aligned}$$

Since an operator for the biharmonic operator for the central node is desired, this expression is evaluated at x_{13}, y_{13}.

$$\begin{aligned} \nabla^4(P(x,y)) &= <\nabla^4\ (V_i(x,y))>\ [M]^{-1}\ \{F_i\} \qquad i=1,2,\ldots,25 \qquad (17) \\ &= <K_i>\ \ \{F_i\} \qquad i=1,2,\ldots,25 \qquad (18) \end{aligned}$$

where $<K_i>$ is a row vector of constants obtained by multiplying the matrix expressions appearing in equation (17). The result is that K_i are the coefficients of a finite difference approximation for the biharmonic operator applied at the central node of the grid in Figure 4.

In order to ensure geometric consistency, this same interpolating polynomial was used to develop the operators appearing on the left hand side of equation (10). The desired operator is applied to the polynomial, and evaluated at the central node. The results for $\alpha = 5$ are presented in Figures 5, 6, and 7, where α is the ratio of the spacing in the x-direction to the spacing in the y-direction.

A finite difference approximation for the harmonic operator, which is required in equation (11) is available in the literature [12]. Consistent approximation for the other operators appearing in this equation are also available. These operators are presented in Figures 8 and 9.

B. BOUNDARY CONDITIONS IN FINITE DIFFERENCE FORM

Assuming there is no jet present, the boundary conditions for ψ^* are all of the form

$$\psi^* = f(t)$$

$$\frac{\partial \psi^*}{\partial n} = g(t)$$

where t is the space coordinate tangent to the boundary,

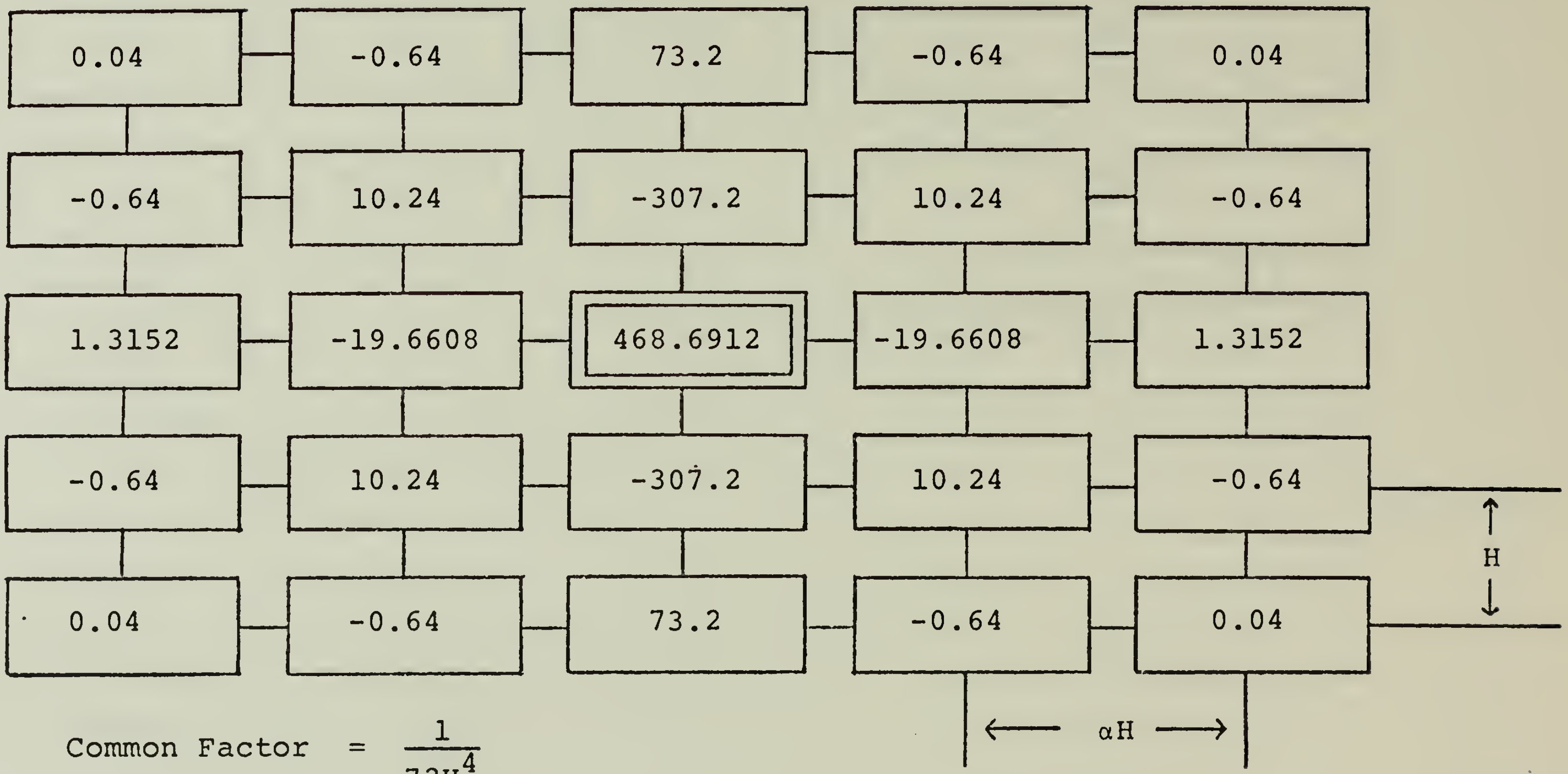

0.04	-0.64	73.2	-0.64	0.04
-0.64	10.24	-307.2	10.24	-0.64
1.3152	-19.6608	$\boxed{468.6912}$	-19.6608	1.3152
-0.64	10.24	-307.2	10.24	-0.64
0.04	-0.64	73.2	-0.64	0.04

Common Factor $= \dfrac{1}{72H^4}$

Truncation Error $= \mathcal{O}\left(\dfrac{1}{H^2} + \dfrac{1}{\alpha^2 H^2}\right)$

Figure 5 - Finite difference approximation for ∇^4 operator for uniform rectangular grid (α=5), applicable at central node.

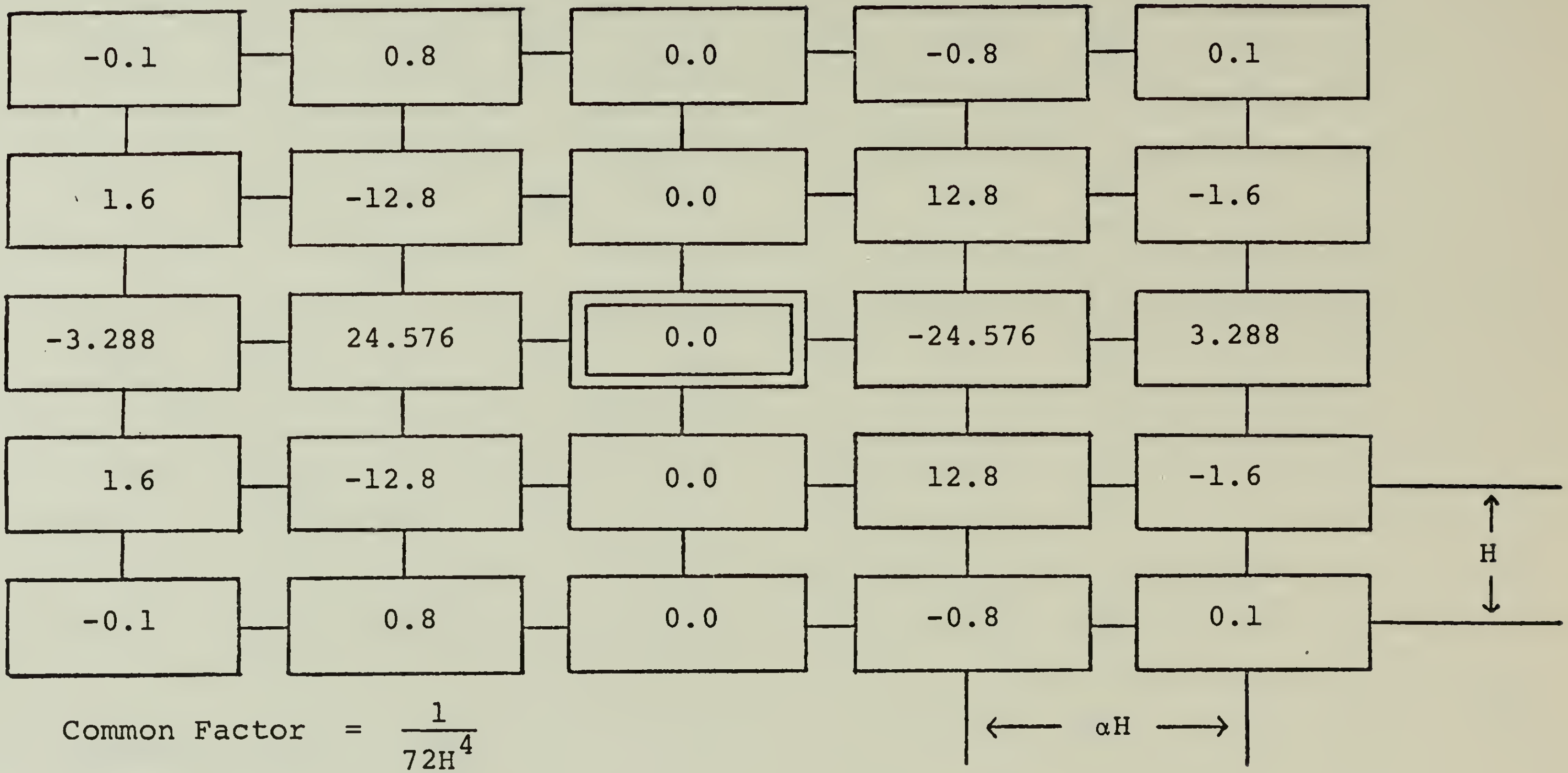

-0.1	0.8	0.0	-0.8	0.1
1.6	-12.8	0.0	12.8	-1.6
-3.288	24.576	$\boxed{0.0}$	-24.576	3.288
1.6	-12.8	0.0	12.8	-1.6
-0.1	0.8	0.0	-0.8	0.1

Common Factor = $\frac{1}{72H^4}$

Figure 6 - Finite difference approximation for the operator $\partial/\partial x(\nabla^2)$ for uniform rectangular grid (α=5), applicable at central node.

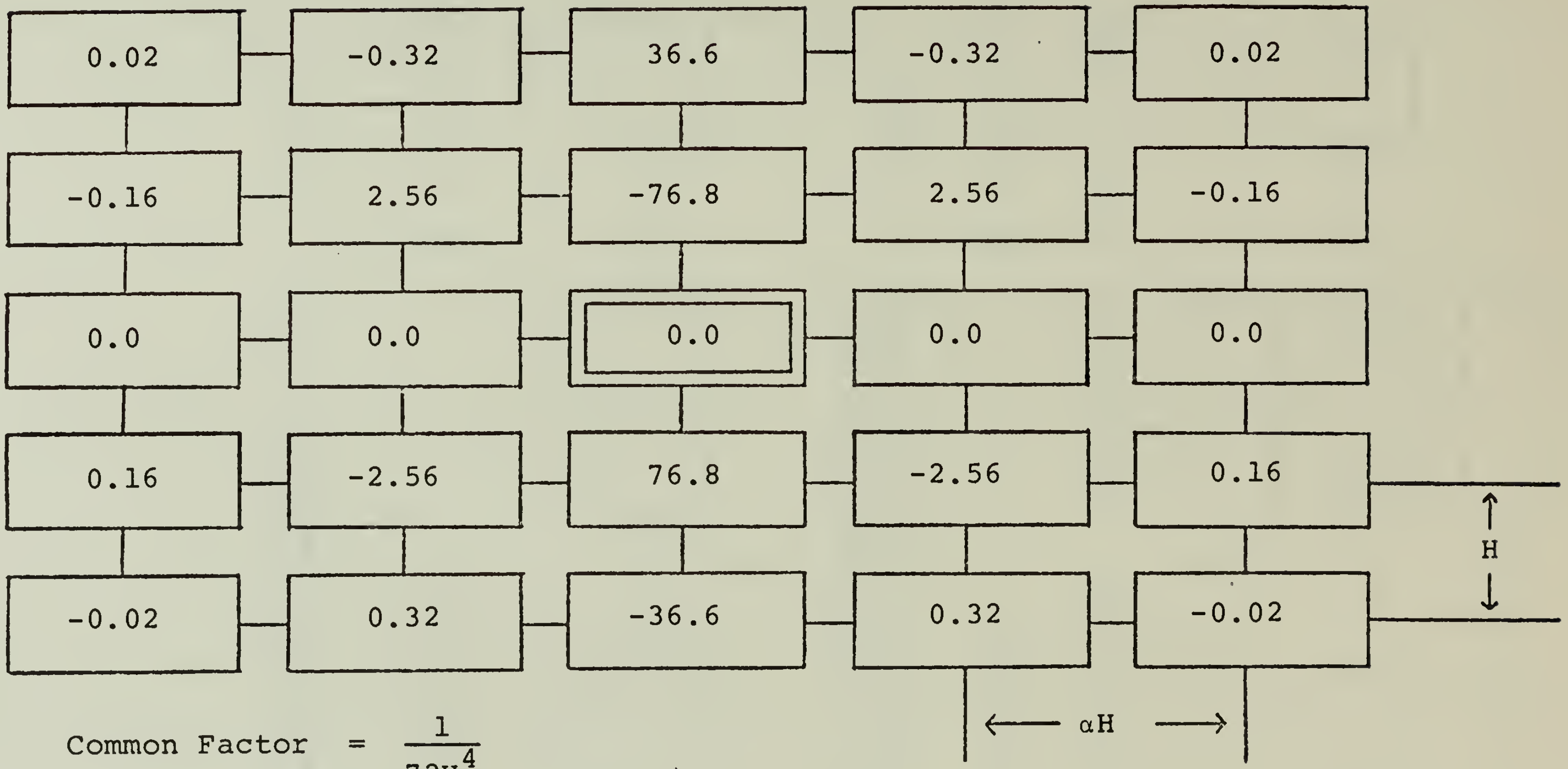

0.02	-0.32	36.6	-0.32	0.02
-0.16	2.56	-76.8	2.56	-0.16
0.0	0.0	0.0	0.0	0.0
0.16	-2.56	76.8	-2.56	0.16
-0.02	0.32	-36.6	0.32	-0.02

Common Factor $= \frac{1}{72H^4}$

Figure 7 - Finite Difference approximation for the operator $\partial/\partial y(\nabla^2)$ for uniform rectangular grid ($\alpha=5$), applicable at central node.

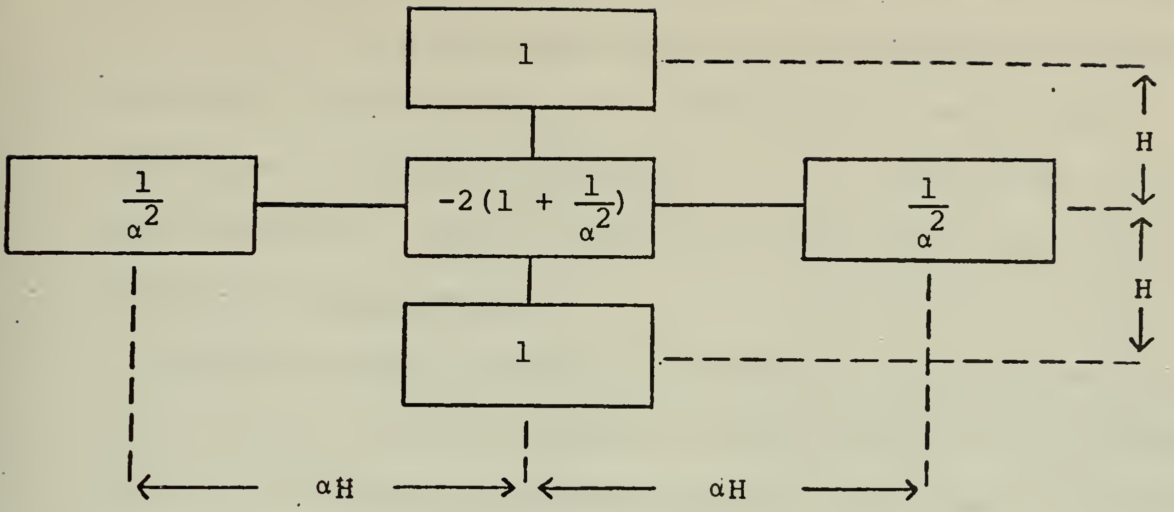

Common Factor = $\frac{1}{H^2}$

Truncation Error = $\mathcal{O}(H^2+\alpha^2H^2)$

Figure 8 - Finite difference approximation for ∇^2 operator applicable at central node

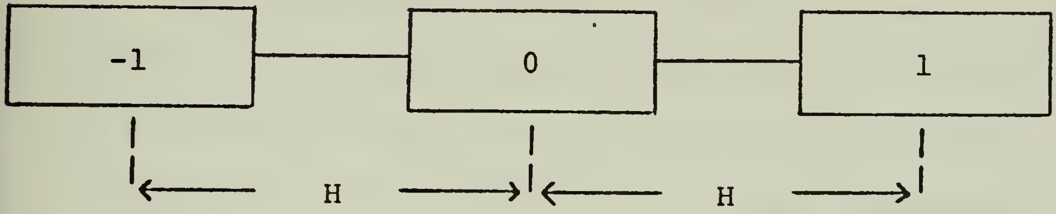

Common Factor = $\frac{1}{2H}$

Truncation Error = $\mathcal{O}(H^2)$

Figure 9 - Finite difference approximation for $\partial/\partial X$ or $\partial/\partial Y$ applicable at central node

n is the coordinate normal to the boundary, and f (t) and g (t) are the values specified at each particular boundary. The first condition on ψ^* is satisfied in the finite difference scheme by evaluating f (t) at each node on the given boundary. These values are then used in the finite difference computations.

To satisfy the boundary condition for the normal derivative of ψ, g (t) is evaluated at each node on the boundary. A finite difference approximation for the normal derivative is then required. An offset three point operator is used because the truncation error is consistent with the truncation error of the governing equation. The finite difference operators used at the boundaries are presented in Figures 10 and 11.

The temperature boundary conditions assume various forms. At the upstream and downstream boundaries, the value of the temperature at the boundary is specified. At nodes located on these boundaries, the known value of the temperature is used in the finite difference computations. On the channel bottom, the derivative of the temperature is specified. At nodes on this boundary, the offset three point operator utilized previously is applied. At the channel surface, the sum of the temperature and its derivative is specified. At nodes on the channel surface, a mixed boundary condition exists. In this case, the value of the temperature at the node located on the surface is added to the three point operator shown in Figure 11.

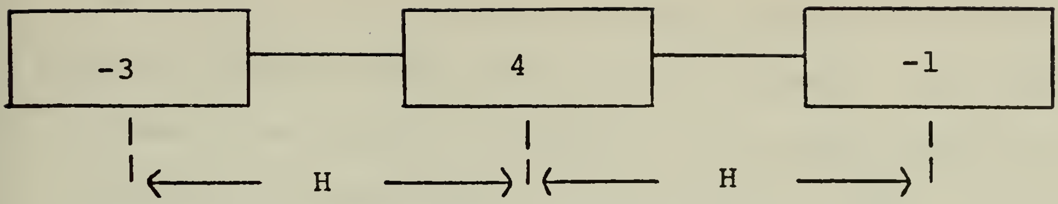

Common Factor = $\frac{1}{2H}$ Truncation Error = $\mathcal{O}(H^2)$

Figure 10 - Finite difference approximation for $\partial/\partial X$ or $\partial/\partial Y$ applicable at first node

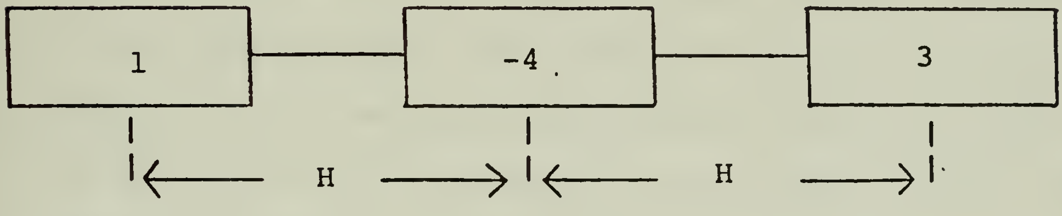

Common Factor = $\frac{1}{2H}$ Truncation Error = $\mathcal{O}(H^2)$

Figure 11 - Finite difference approximation for $\partial/\partial x$ or $\partial/\partial Y$ applicable at last node

For most computations, the jet center is located between two nodes. In addition, the jet diameter is assumed to be less than the grid spacing in all cases. The effective diameter of the jet is equal to the grid spacing on the boundary on which the jet is located. This is a result of the fact that any length smaller than the grid spacing cannot be accurately modeled in a finite difference network. This can best be illustrated by example. Figure 12 depicts two possible jet configurations, both having the same volume flow rate. Also shown are the stream function profiles, superimposed on a grid network. In both cases, the jet width is less than the grid spacing. It can be readily seen that the values of the stream function at the two nodes on either side of the jet are the same, regardless of the jet diameter. The value of the stream functin is changed by the amount of the volume flow rate of the jet. If the jet width is smaller than the grid spacing, the effect of the jet on the finite difference grid is a fixed flow rate between two grid points. The effective diameter of the jet is then equal to the grid spacing, and the effective jet velocity is the flow rate divided by the grid spacing.

By modeling the jet in this manner, the edges of the jet fall on nodes of the finite difference grid. In a continuous system, there is a step change in both the temperature profile and the velocity profile at these points. This step change cannot be modeled precisely in a

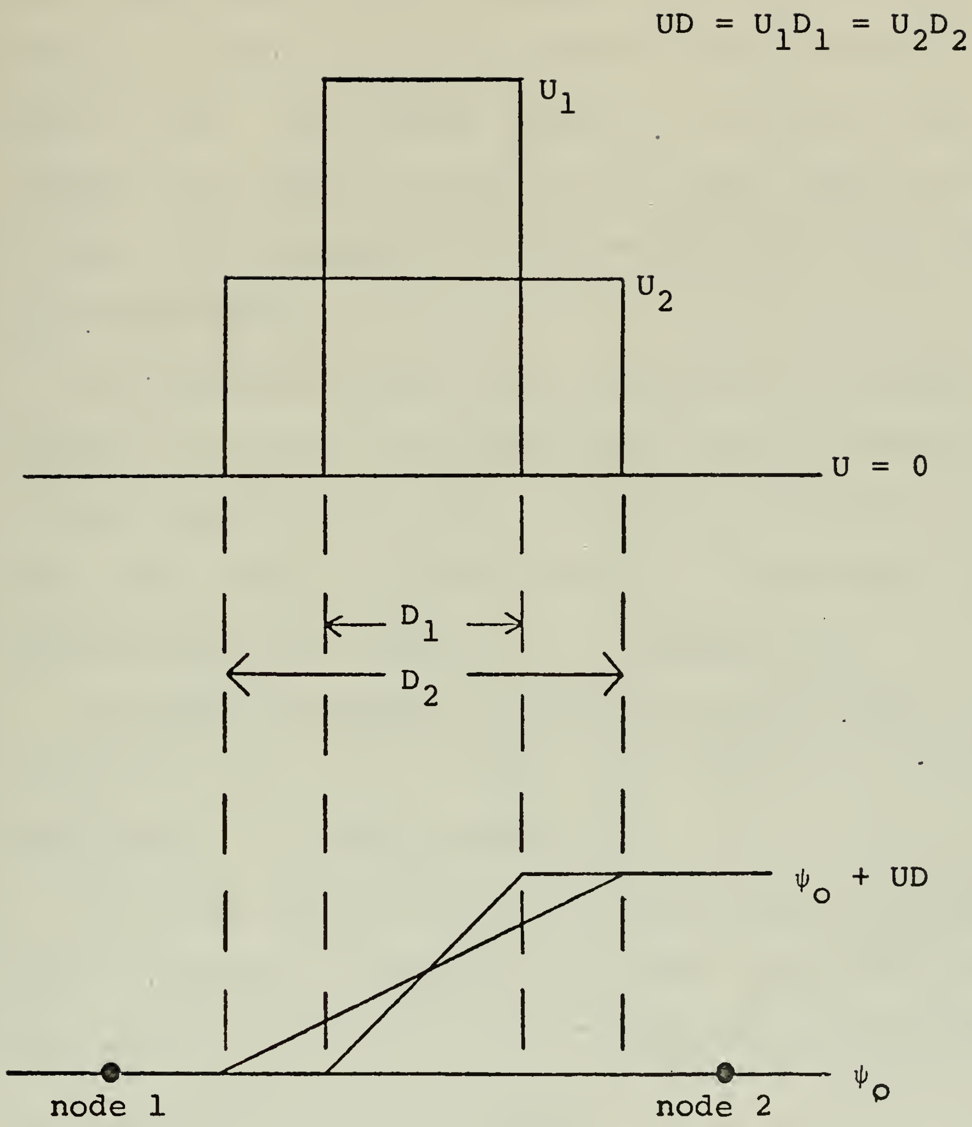

Figure 12 - Velocity profiles and resulting stream function profiles for two jets located between nodes 1 and 2.

finite difference scheme. By specifying the temperature at these two nodes in the finite difference grid, the temperature profile is as shown in Figure 13. It can be seen that the total area under the temperature profile curve is equal to the area under a step change of temperature $2 \times T_S$. The energy input of the profile shown in Figure 13 is equal to that of the step change of height $2 \times T_S$. This temperature may be defined as the effective jet temperature.

If the three point finite difference operator shown in Figure 9 is used to calculate the velocity profile based on the relation $V = \frac{\partial \psi^*}{\partial Y}$, it can be shown that the effective jet velocity defined earlier is consistent with the definition of the effective jet temperature.

The above examples are directly applicable to the transverse jet. By analogy, the results may easily be extended to the longitudinal jet.

For the results used to construct the convergence plot, the jet center is located at a node. For this orientation, the effective jet diameter is twice the grid spacing.

C. NUMERICAL SOLUTION SCHEME

In the numerical solution of this problem, the governing equations are rearranged

$$\nabla^4 \psi^* = -\frac{Gr}{Re}\frac{\partial \theta}{\partial X} + \left[\frac{\partial \psi^*}{\partial Y}\frac{\partial (\nabla^2 \psi^*)}{\partial X} - \frac{\partial \psi^*}{\partial X}\frac{\partial (\nabla^2 \psi^*)}{\partial Y}\right] Re \tag{18}$$

$$\nabla^2 \theta = RePr \left[\frac{\partial \psi}{\partial Y}\frac{\partial \theta}{\partial X} - \frac{\partial \psi}{\partial X}\frac{\partial \theta}{\partial Y}\right] \tag{19}$$

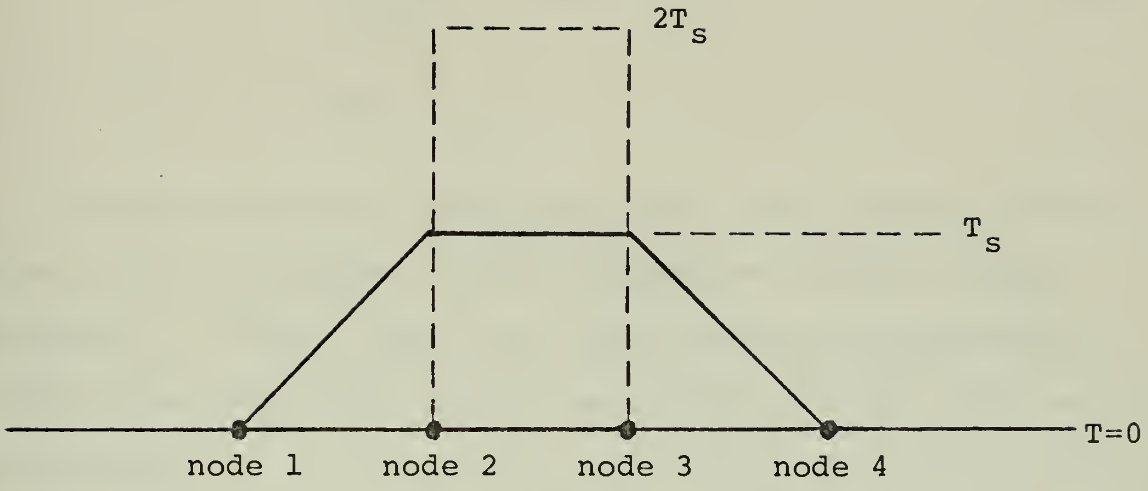

Figure 13 - Temperature profile over finite difference grid in the vicinity of the transverse jet.

These equations may be expressed in an alternate form if we recognize that the Jacobian operator is defined as

$$J(A,B) = \frac{\partial A}{\partial X}\frac{\partial B}{\partial Y} - \frac{\partial A}{\partial Y}\frac{\partial B}{\partial X}$$

Equations (1) and (2) may then be rewritten as:

$$\nabla^4\psi^* = -\frac{Gr}{Re}\frac{\partial\theta}{\partial X} - J(\psi^*,\nabla^2\psi^*)Re \qquad (20)$$

$$\nabla^2\theta = RePr\ J(\psi^*,\theta) \qquad (21)$$

In the solution of these equations, an iterative scheme based on the uncoupled linear homogeneous forms of these equations is used. Once this linear system of equations is solved, the right hand side of equations (20) and (21) may be calculated.

The linear equations are then resolved, using the calculated values of the right hand side of the equations as known inhomogeneities. This procedure is repeated until the desired convergence criteria is satisfied.

The uncoupled linear homogeneous forms of equations (20) and (21) are:

$$\nabla^4\psi^* = 0$$

$$\nabla^4\theta = 0$$

The method of solving these equations with the boundary conditions for the transverse will be illustrated using the grid in Figure 14 as an example.

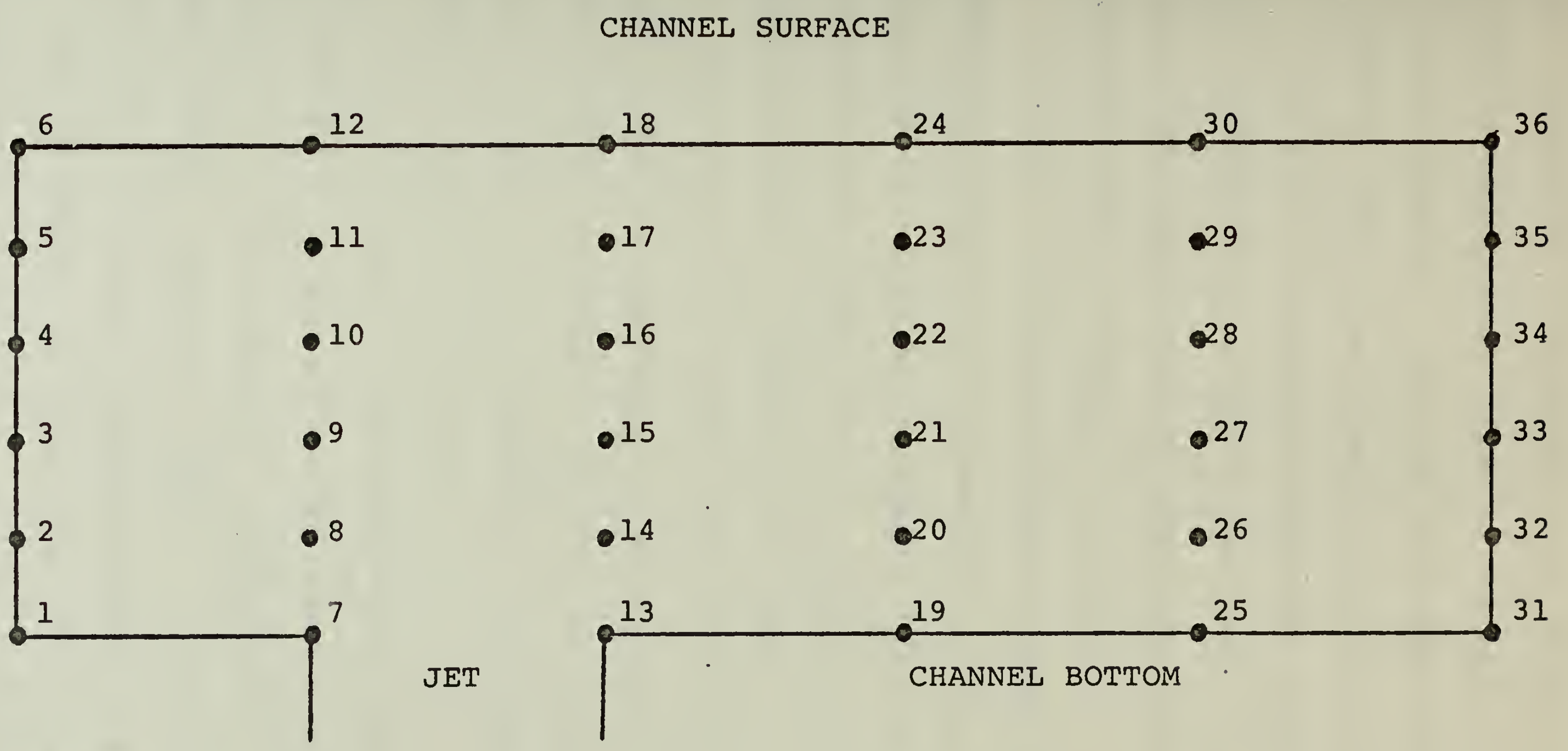

Figure 14 - Typical grid network.

The boundary conditions on ψ^* specify the value of ψ^* on all boundaries. Therefore, the value of ψ^* at nodes located on the boundaries is known. The value of ψ^* at each interior node is unknown. In order to solve for the value of ψ^* at interior nodes, one equation for each node is required.

For all ψ^* values not adjacent to any boundary (nodes 15, 16, 21, and 22 in example), an equation is obtained by applying the governing equation at the node. The finite difference operator shown in Figure 5 is used.

For all ψ^* values located at nodes adjacent to the upstream boundary (nodes 8-11 in example), an equation is obtained by applying the boundary condition $\frac{\partial \psi^*}{\partial X} = 0$ at the adjacent boundary node (nodes 2-5 in example). The finite difference operator shown in Figure 10 is used.

For ψ^* values at nodes adjacent to the downstream boundary (nodes 26-29 in example), an equation is obtained by applying the boundary condition $\frac{\partial \psi^*}{\partial X} = 0$ at the adjacent boundary node (nodes 32-35 in example). The finite difference operator shown in Figure 11 is used.

For ψ^* values at nodes adjacent to the channel bottom, but not adjacent to either the upstream or downstream boundary (nodes 12, 20 in example), an equation is obtained by applying the boundary condition $\frac{\partial \psi^*}{\partial Y} = 0$ at the adjacent boundary node. The finite difference operator shown in Figure 10 is used.

For ψ^* values at nodes adjacent to the channel surface, but not adjacent to either the upstream or downstream boundary, (nodes 17, 23 in example), an equation is obtained by applying

the boundary condition $\frac{\partial \psi^*}{\partial Y} = \frac{9}{7}$ at the adjacent boundary node (nodes 13, 19 in example). The finite difference operator shown in Figure 11 is used.

Since the value of ψ^* is known at nodes located on the boundary, whenever a finite difference operator involves the value of ψ^* on a boundary, the known value of ψ^* is used. The resulting system of equations is a set of algebraic equations for each unknown. This system of equations is solved by Gaussian elimination.

The boundary conditions for θ specify the value of θ at the upstream and downstream boundaries, and at the two nodes on either side of the jet. However, the value of the temperature on the channel surface is unknown, and the value of the temperature on the channel bottom, except for the nodes on either side of the jet, is also unknown. Again, one equation for each unknown is required.

For each θ unknown not located on a boundary (nodes 8-11, 14-17, 20-23, 26-29 in example), the equation $\nabla^2\theta = 0$ is applied at the node at which the unknown is located. The finite difference operator shown in Figure 8 is used.

For θ unknowns located at nodes on the channel bottom (nodes 19-25 in example), an equation is obtained by applying the boundary condition $\frac{\partial \theta}{\partial Y} = 0$ at the node. The finite difference operator shown in Figure 10 is used.

For θ unknowns located at the channel surface, (nodes 12, 18, 24, 30 in example), an equation is obtained by applying the boundary conditions $\frac{\partial \theta}{\partial Y} + \frac{hD}{K}\theta = 0$ at the node. The finite difference operator shown in Figure 11 is used.

The result is an equation for each θ unknown. This system of equations is solved using Gaussian elimination methods.

The method of solving equations (20) and (21) is presented in the form of a flow chart in Figure 15. The superscripts, e.g., $\psi^{*\ell}$ refer to the solutions at every node on the ℓ^{th} iteration in a particular loop. The quantity $R_S(\psi^{*m},\theta^n)$ is defined as the right hand side of equation (20) based on the known values of ψ^{*m} and θ^n. The quantity R_θ is the right hand side of equation (21) defined similarly.

The convergence tests for ψ^* and θ are:

$$\left|\frac{\psi^{i-1} - \psi^{i}}{\psi^{i-1}}\right| < 0.001$$

$$\left|\frac{\theta^{i-1} - \theta^{i}}{\theta^{i-1}}\right| < 0.001$$

It is assumed that when the above criteria are satisfied at every node, the solution has converged.

It should be pointed out that the governing equation is not applied at every unknown node. The non-linear terms calculated from the values of functions from the previous iteration affect the known value in the governing equation only at nodes at which the governing equation is applied. However, the solution for every node is affected, because the equations are solved simultaneously by Gaussian elimination techniques.

In the calculation of the right hand sides of equations (20) and (21), two different techniques were used. The first

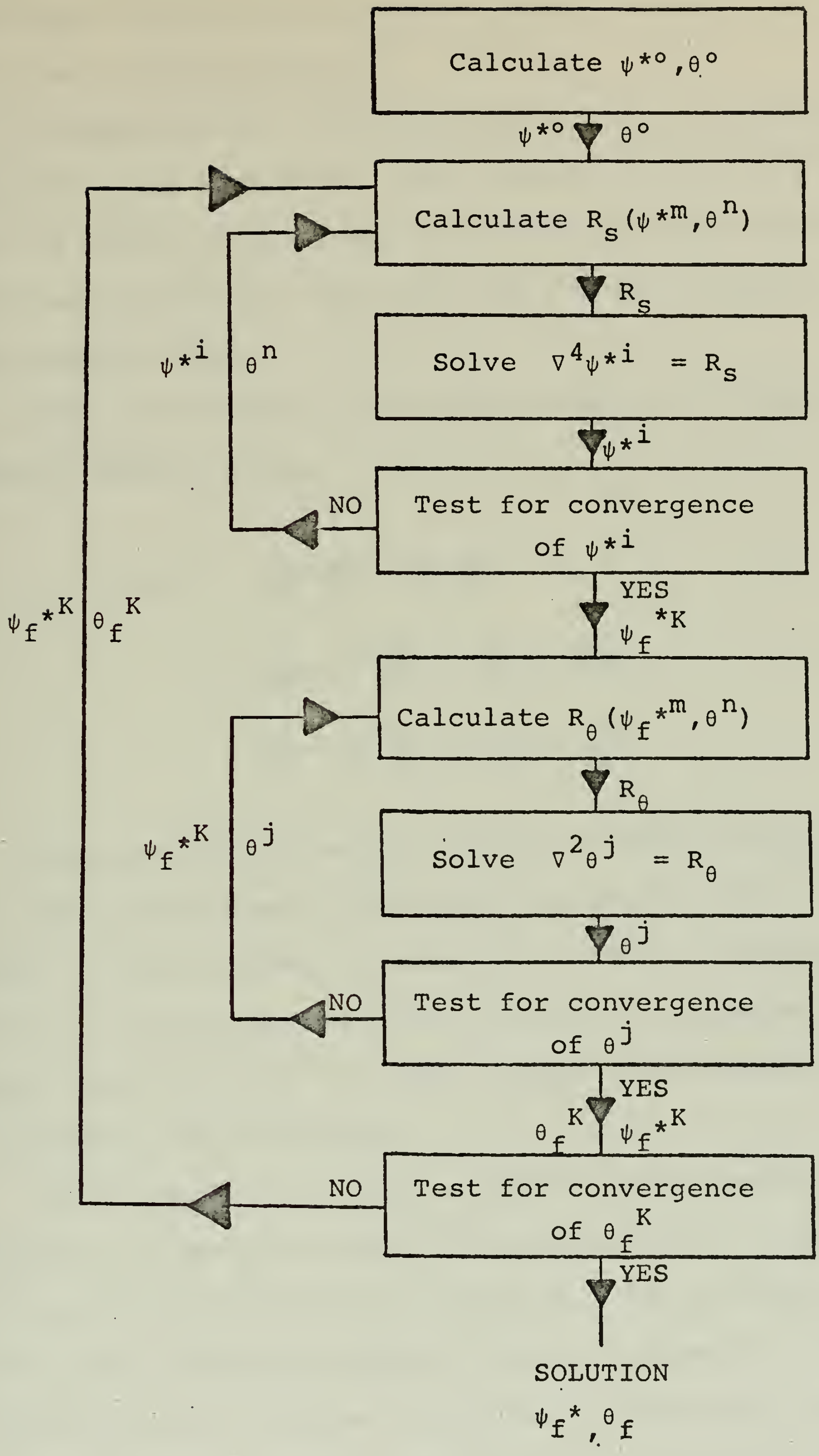

Figure 15 - Flow chart for iterative scheme.

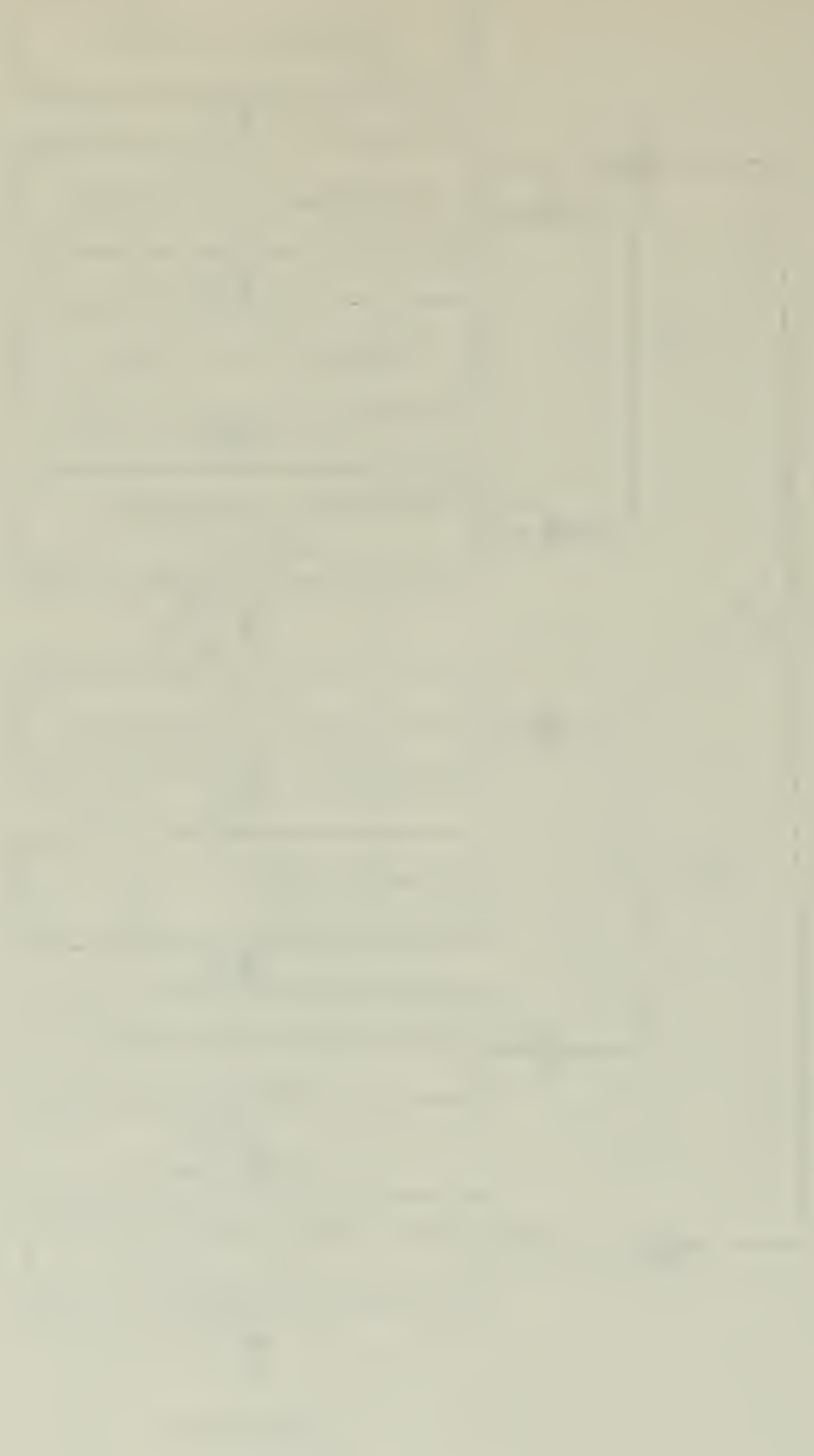

technique utilized the operators shown in Figure 6, 7, and 9, which were derived earlier.

A second method , which provided improved numerical stability, was also used. This method is described in [13]. This is simply an alternate way of calculating the Jacobian, which appears both in the right hand side of equation (20) and equation (21).

Using this method, the Jacobian Operator is expressed in three alternate forms:

$$\begin{aligned} J(A,B) &= \frac{\partial A}{\partial X}\frac{\partial B}{\partial Y} - \frac{\partial A}{\partial Y}\frac{\partial B}{\partial X} \\ &= \frac{\partial}{\partial X}\left(A\frac{\partial B}{\partial Y}\right) - \frac{\partial}{\partial Y}\left(A\frac{\partial B}{\partial X}\right) \\ &= \frac{\partial}{\partial Y}\left(B\frac{\partial A}{\partial X}\right) - \frac{\partial}{\partial X}\left(B\frac{\partial A}{\partial Y}\right) \end{aligned}$$

When the quantities are grouped in this manner, applying the three point central difference operator shown in Figure 9 leads to three different numerical methods of calculating J(A,B). By calculating J(A,B) by each of these methods, and using the average of the three values, some forms of numerical instability are eliminated.

This method may be applied directly to equation (20). However, in order to apply it to equation (21), the value of $\nabla^2\psi^*$ must be calculated at each node. This is done by applying the finite difference operator shown in Figure 8. The method described above can then be applied to calculate $J(\psi^*,\nabla^2\psi^*)$.

The computer program used to obatin the results which are presented is included in Appendix B.

IV. RESULTS

A. PRESENTATION OF RESULTS

In the results, velocity data are presented in the form of streamlines in the channel. Temperature data are presented in the form of isotherms in the channel. Both the streamlines and the isotherms are presented in non-dimensional form, and are plotted with respect to non-dimensional values X and Y. These graphs are based on linear interpolation between calculated values of ψ^* and θ at nodes in the grid. It should be noted that in the graphical plots for both ψ^* and θ, the scale in the Y-direction is twice that in the X-direction. The grid used for all calculations consisted of 7 nodes in the Y-direction and 19 in the X-direction.

For all results presented, the surface boundary condition on the temperature is $\frac{\partial\theta}{\partial Y} + \frac{hD}{k}\,\theta = 0$. Additionally, the ratio of the flow rate of the jet to the flow rate of the river is 0.2 in all cases. This value was chosen as a representative value for an actual power plant, and was felt to be small enough so that the surface boundary condition on the vertical velocity (i.e., no waves) remains valid.

In Figures 16-21, the streamlines and isotherms for a transverse jet of width 5D/6 are presented. The Reynolds number and Prandtl for all these figures are Re = 0.3 and Pr = 6.0. Results for three different values of the ratio of the Grashof number to the Reynolds number are presented;

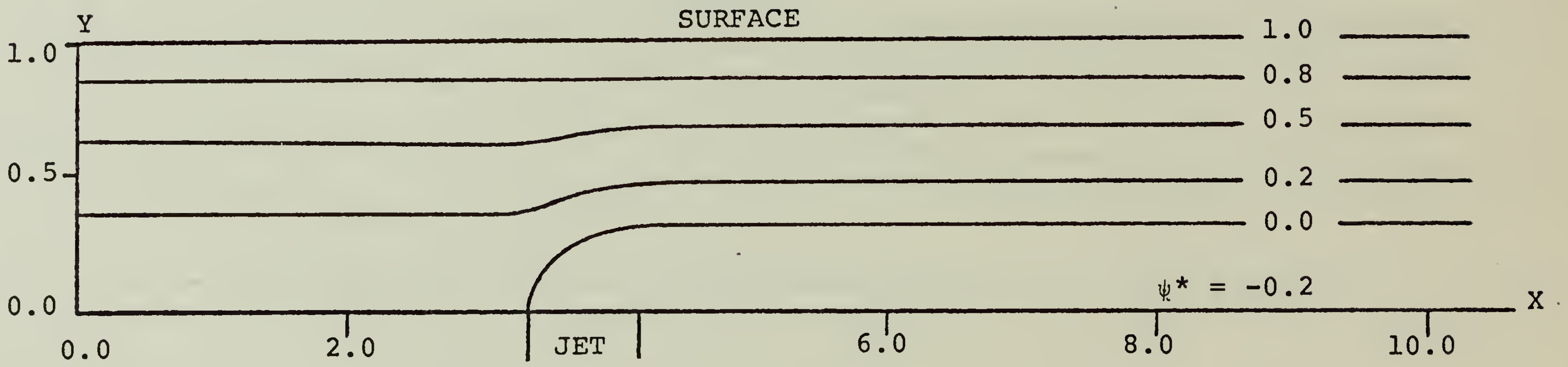

Figure 16 - Streamlines for a transverse of width 5D/6, Gr/Re = 0.0, Re = 0.3, Pr = 6.0, $U_j D_j^* = 0.2$.

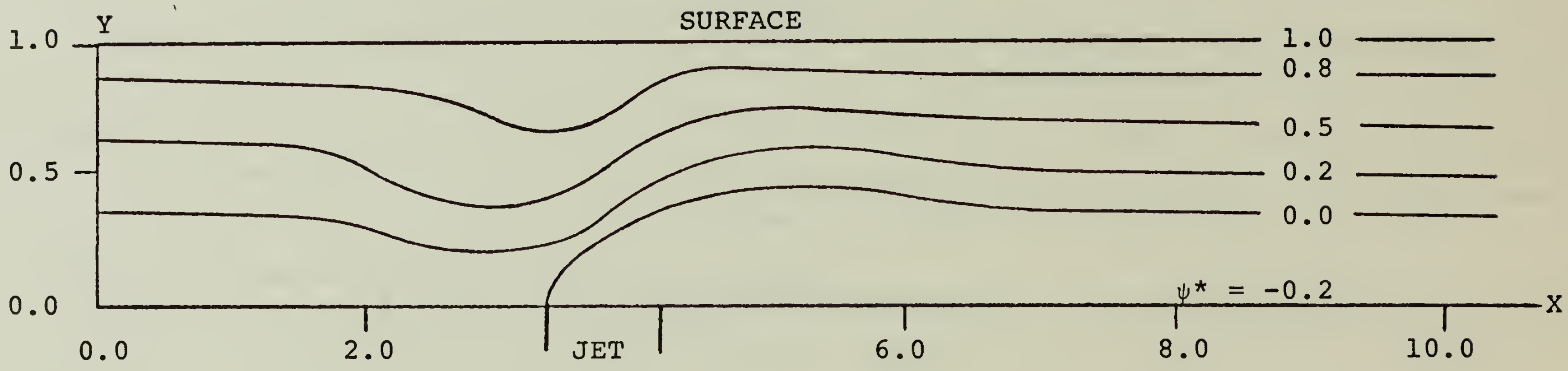

Figure 17 - Streamlines for a transverse jet of width 5D/6, Gr/Re = 600.0, Re = 0.3, Pr = 6.0, $U_jD_j^* = 0.2$.

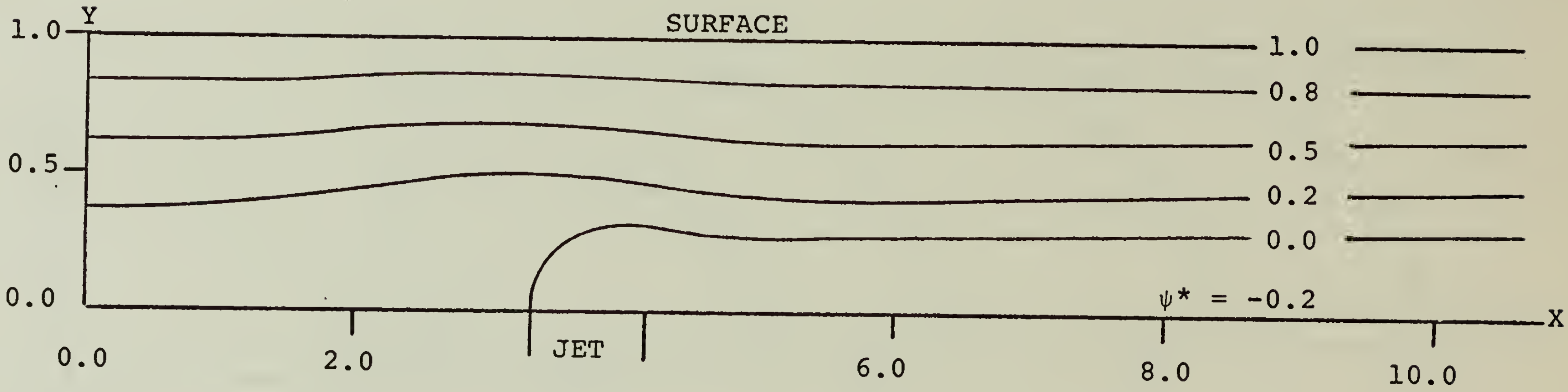

Figure 18 - Streamlines for transverse jet of width 5D/6, Gr/Re = -300.0, Re = 0.3, Pr = 6.0, $U_jD_j^* = 0.2$.

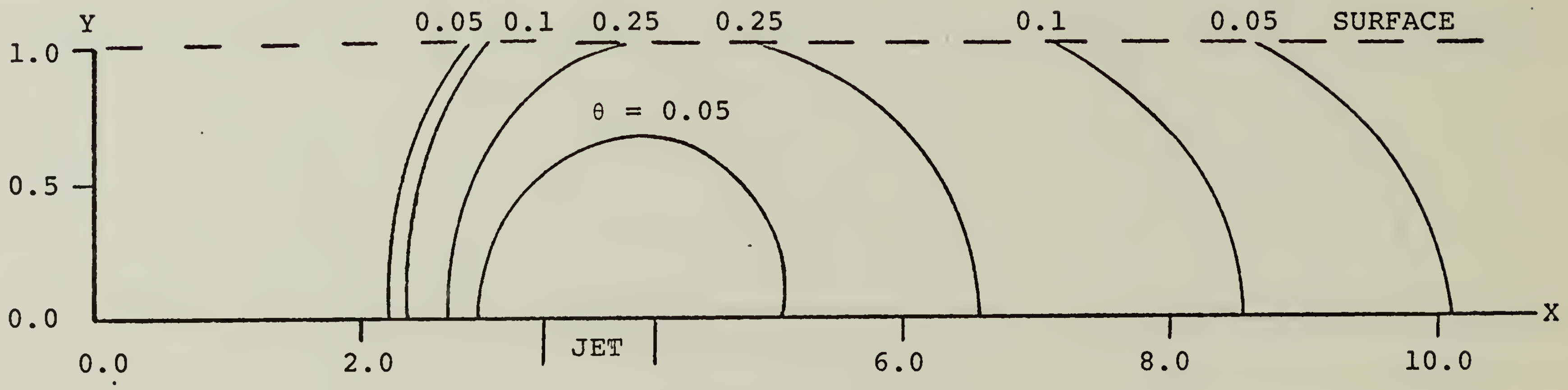

Figure 19 - Isotherms for a transverse jet of width 5D/6, Gr/Re = 0.0, Re = 0.3, Pr = 6.0, $U_j D_j^* = 0.2$.

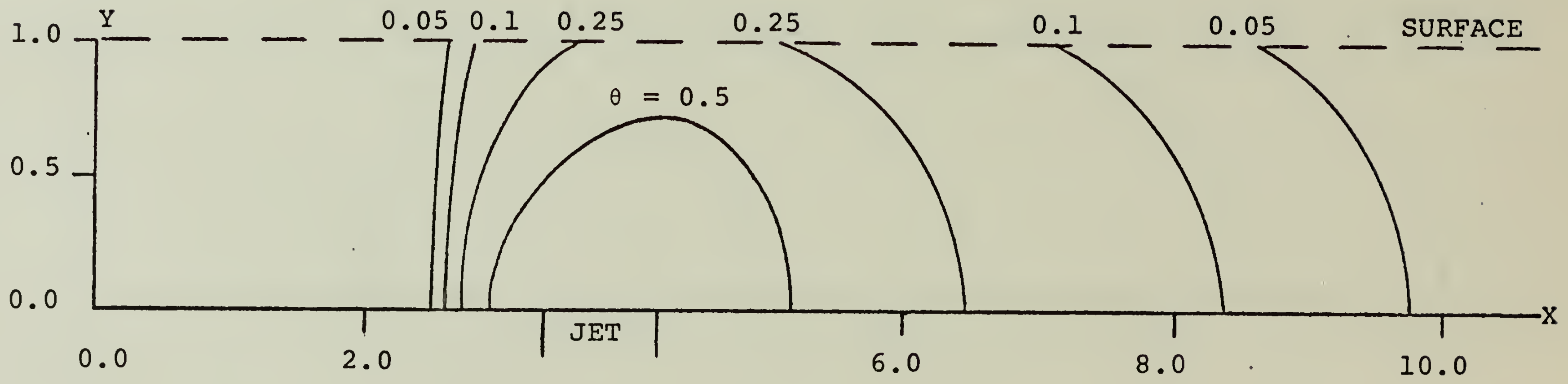

Figure 20 - Isotherms for a transverse of width 5D/6, Gr/Re = 600.0, Re = 0.3, Pr = 6.0, $U_j D_j^* = 0.2$.

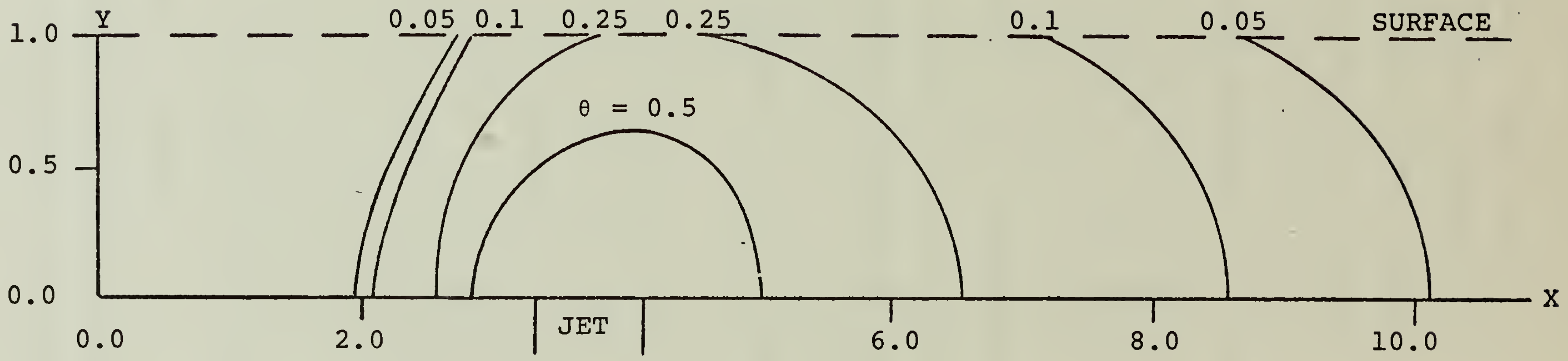

Figure 21 - Isotherms for a transverse jet of width 5D/6, Gr/Re = -300.0, Re = 0.3, Pr = 6.0, $U_j D_j^* = 0.2$.

Gr/Re = 600, Gr/Re = 0, and Gr/Re = -300. The case of a negative value of Gr/Re implies that the temperature of the jet is less than the temperature of the stream. Hence, the buoyant force acts in the opposite direction, i.e., downward.

In Figures 22-27, the streamlines and isotherms for a longitudinal jet of width of D/6 located between Y = 1/3 and Y = 1/2 are presented. For all these figures, Re = 0.3 and Pr = 6.0. The three values of Gr/Re presented are Gr/Re = 600, Gr/Re = 0, and Gr/Re = -300.

In Figures 28-29, the streamlines for both a transverse jet of width 5D/6 and a longitudinal jet of width D/6 between Y = 1/3 and Y = 1/2 are presented. The values of the non-dimensional parameters for these figures Re = 40, Pr = 6.0, and Gr/Re = 0. No isotherms are presented because the jet is assumed to be at the same temperature as the river.

In Figure 30 and Table 1, the surface temperature as a function of X is presented. The temperatures for the longitudinal jet are presented in tabular form becasue differences in the temperatures for the three different values of Gr/Re are difficult to distinguish graphically. For all cases in Figure 30 and Table 1 the Reynolds number and the Prandtl number are Re = 0.3 and Pr = 6.0. The value of Gr/Re for each case is indicated in the results.

B. DISCUSSION OF RESULTS

The effect of the buoyant force on the flow patterns and isotherms can be seen by examining the graphical results in

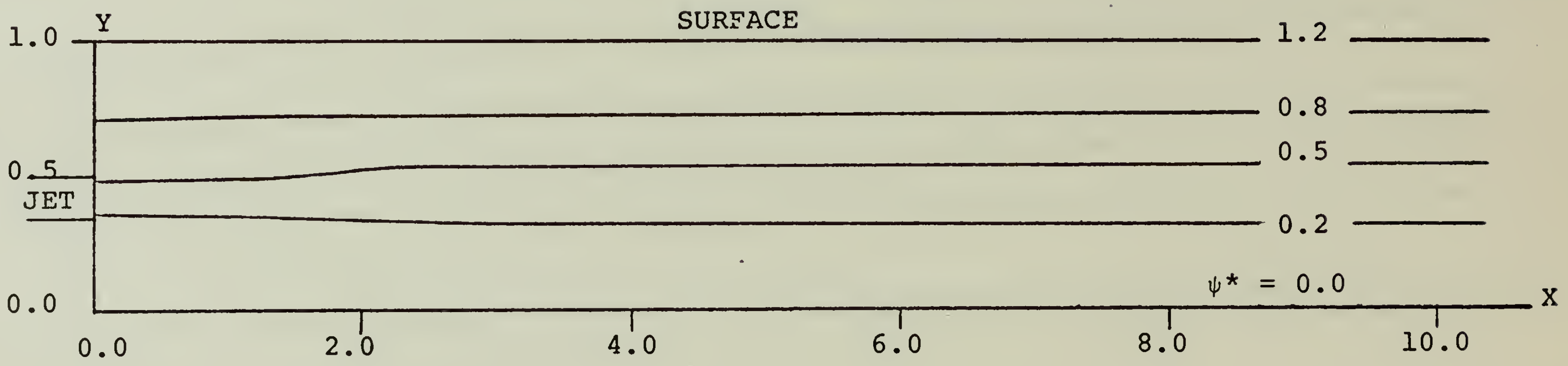

Figure 22 - Streamlines for a longitudinal jet of width D/6, Gr/Re = 0.0, Re = 0.3, Pr = 6.0, $U_jD_j^* = 0.2$.

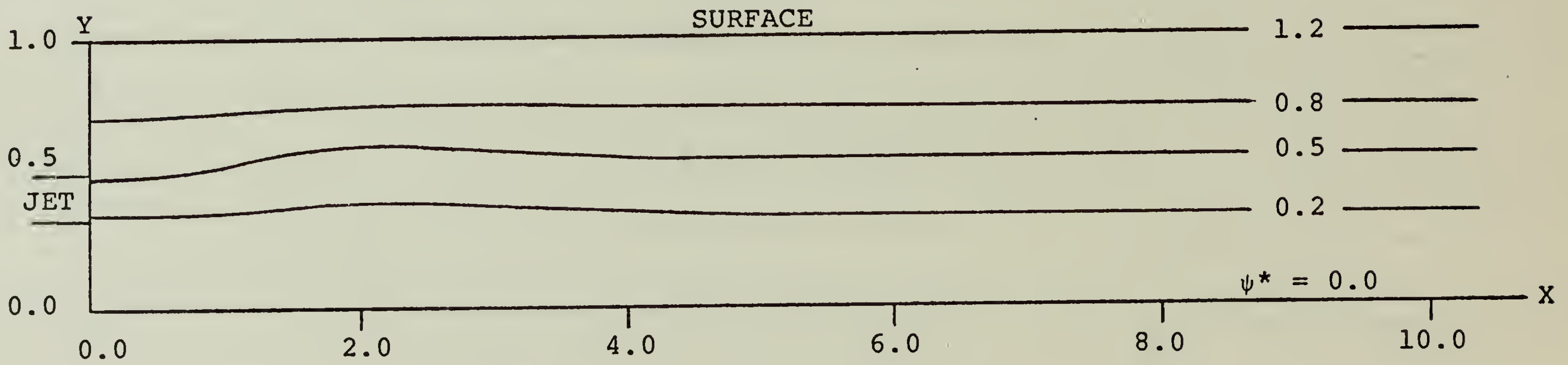

Figure 23 - Streamlines for a longitudinal jet of width D/6, Gr/Re = 600.0, Re = 0.3, Pr = 6.0, $U_j D_j^* = 0.2$.

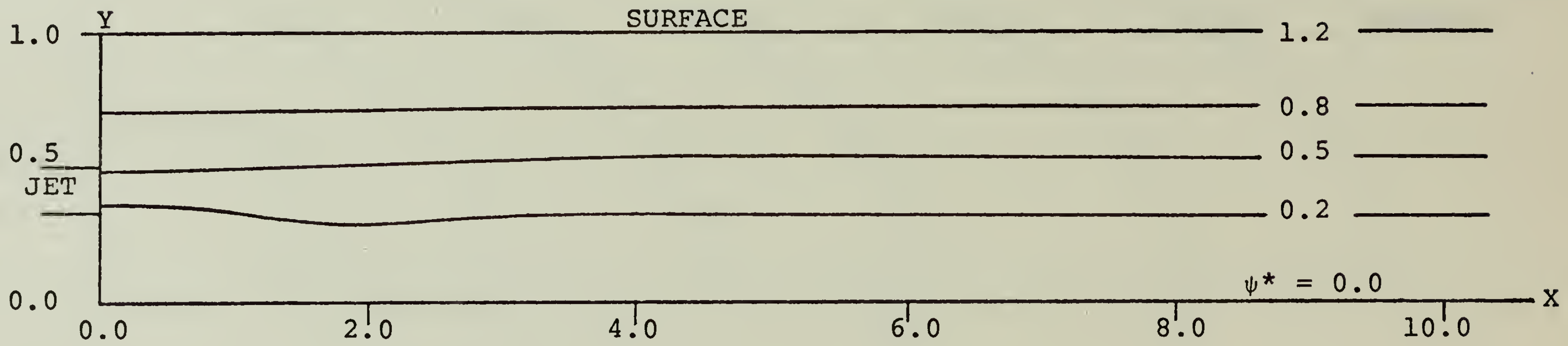

Figure 24 - Streamlines for a longitudinal jet of width D/6, Gr/Re = -300.0, Re = 0.3, Pr = 6.0, $U_j D_j^* = 0.2$.

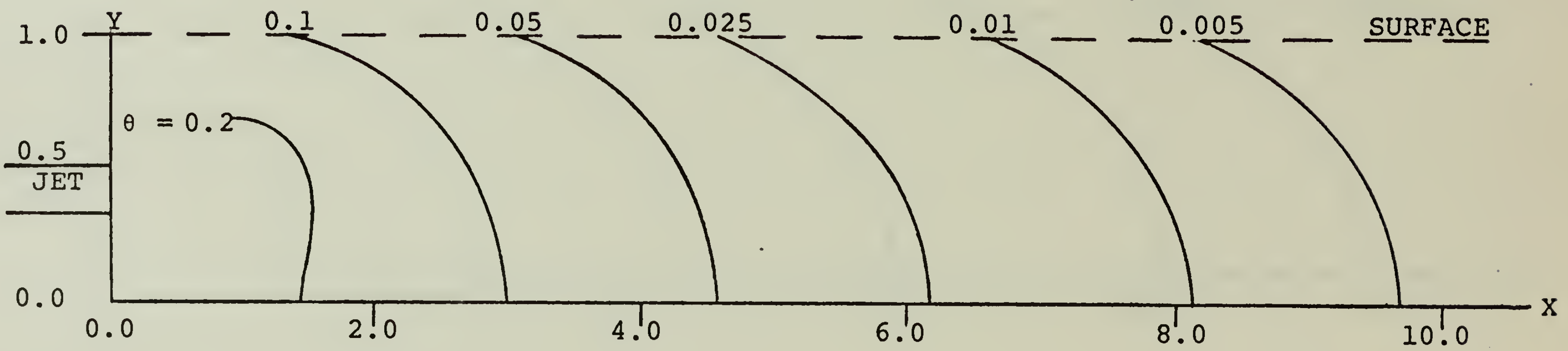

Figure 25 - Isotherms for a longitudinal jet of width D/6, Gr/Re = 0.0, Re = 0.3, Pr = 6.0, $U_j D_j^* = 0.2$.

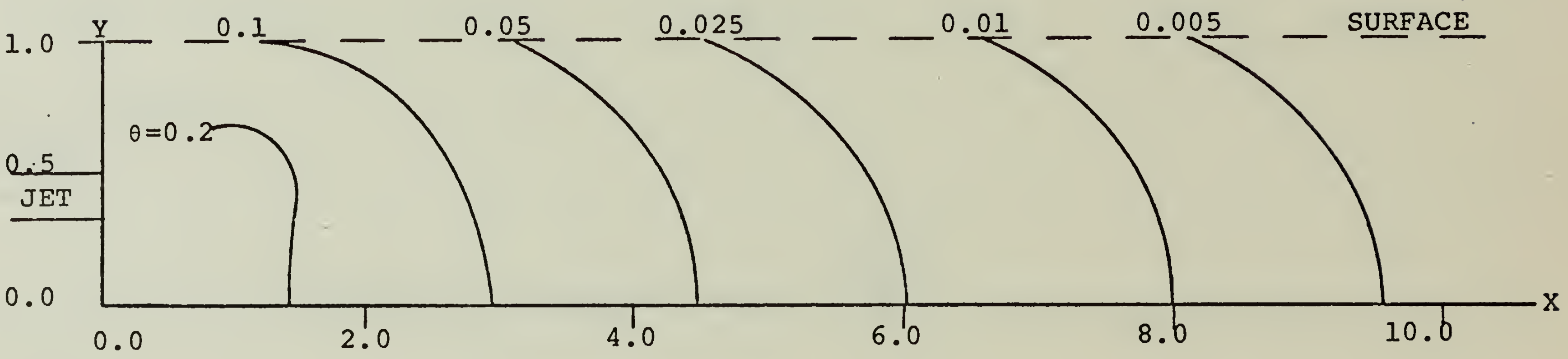

Figure 26 - Isotherms for a longitudinal jet of width D/6, Gr/Re = 600.0, Re = 0.3, Pr = 6.0, $U_j D_j^* = 0.2$.

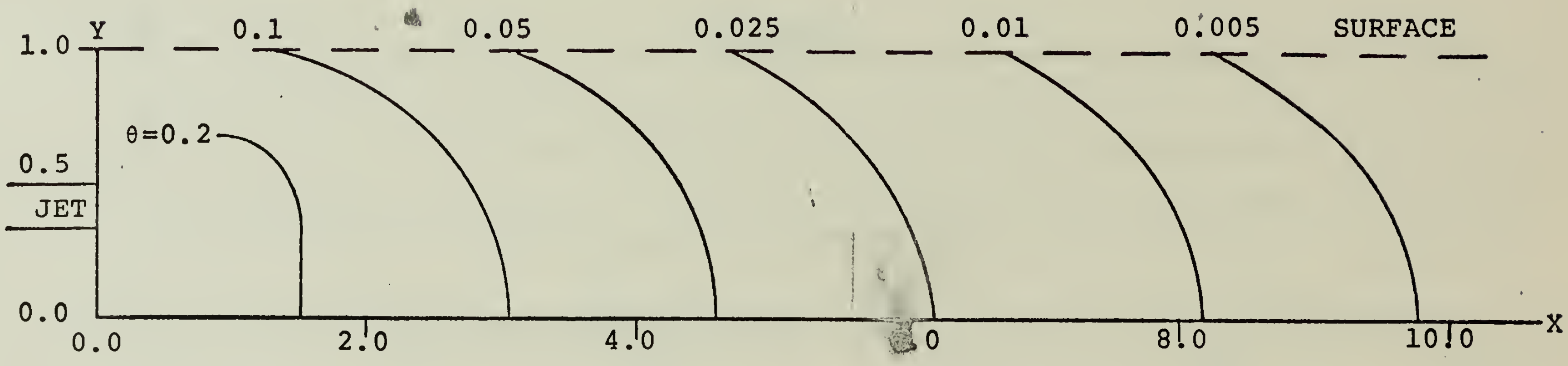

Figure 27 - Isotherms for a longitudinal jet of width D/6, Gr/Re =-300.0, Re = 0.3, Pr = 6.0, $U_jD_j{}^* = 0.2$.

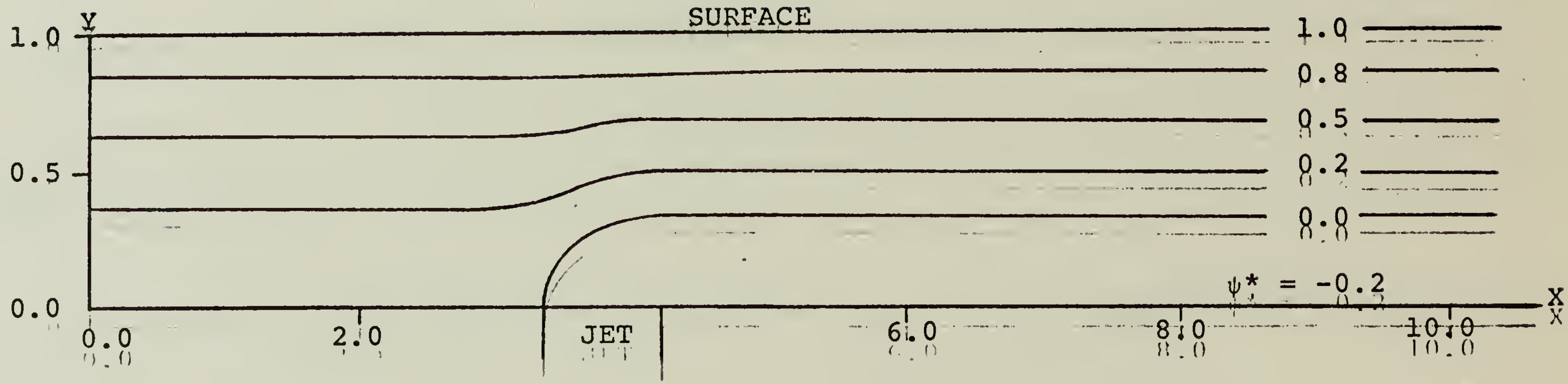

Figure 28 - Streamlines for a transverse jet of width 5D/6, Gr/Re = 0.0, Re = 40.0, Pr = 6.0, $U_j D_j^* = 0.2$.

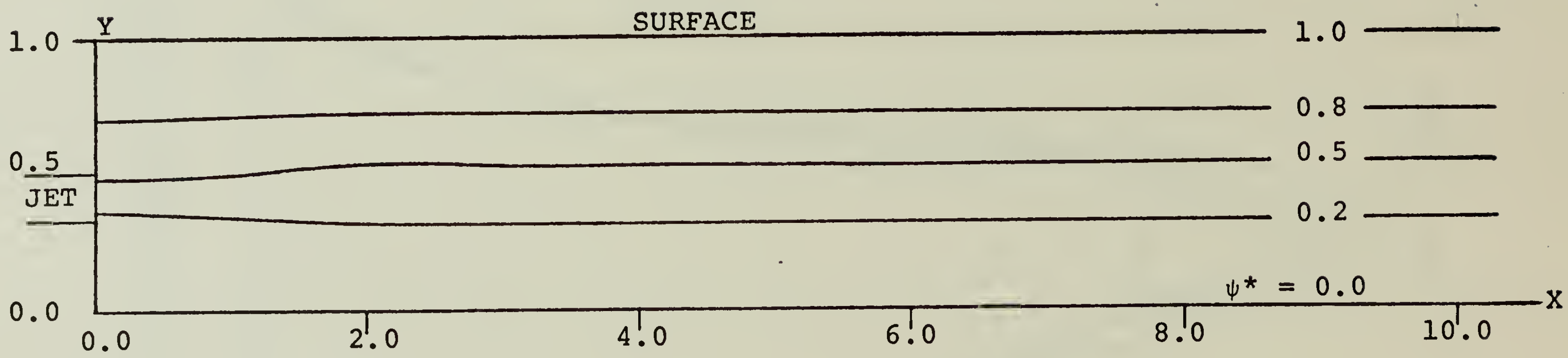

Figure 29 - Streamlines for a longitudinal jet of width D/6, Gr/Re = 0.0, Re = 40.0, Pr = 6.0, $U_j D_j{}^* = 0.2$.

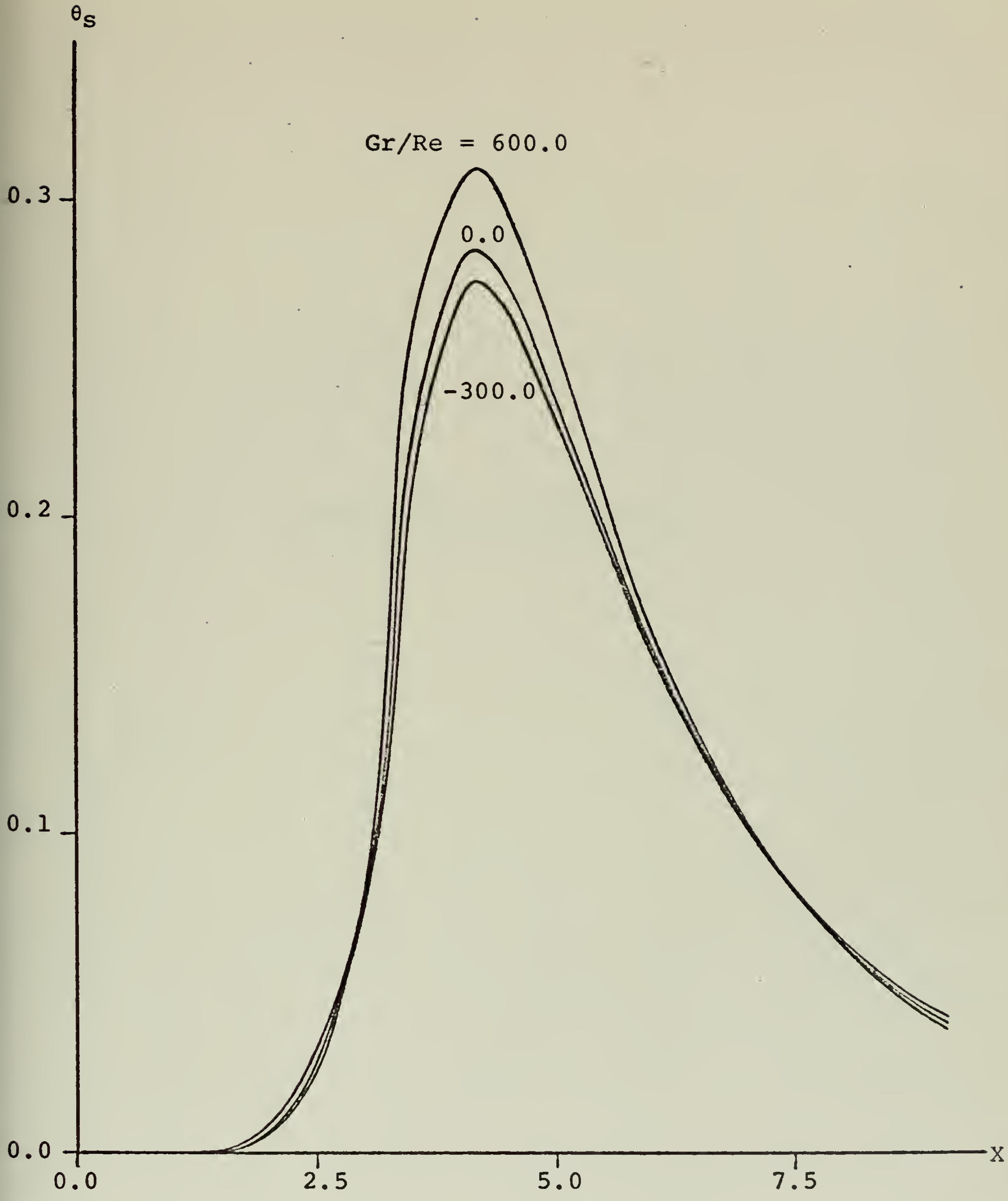

Figure 30 - Surface temperature vs. X for a transverse jet of width 5D/6, Re = 0.3, Pr = 6.0.

(This page intentionally blank)

TABLE I

Surface Temperature (θ_s)

Longitudinal Jet

X	θ_s Gr/Re = 600	θ_s Gr/Re = 0	θ_s Gr/Re = -300
0.0	0.0	0.0	0.0
0.833	0.1083	0.1077	0.1074
1.667	0.0907	0.0901	0.0898
2.500	0.0632	0.0635	0.0636
3.333	0.0431	0.0437	0.0440
4.167	0.0294	0.0300	0.0304
5.000	0.0200	0.0300	0.0304
5.833	0.0137	0.0141	0.0144
6.667	0.0094	0.0097	0.0099
7.500	0.0064	0.0066	0.0067
8.333	0.0044	0.0046	0.0047
9.167	0.0030	0.0031	0.0032
10.000	0.0021	0.0022	0.0022

Figures 16-21 and 22-27. The case of Gr/Re = 0 implies the buoyant effect is negligible in the momentum equation. In this case, no buoyant force acts on the flow, and the momentum equation is independent of the temperature equation. A positive value of Gr/Re implies that the temperature of the jet is greater than T_o. In this case, the buoyant force acts in the positive Y-direction. A negative value of Gr/Re implies that the temperature of the jet is less than T_o. In this case, the buoyant force acts in the negative Y-direction. In order to examine the effect of buoyancy, the cases in which Gr/Re is non-zero are compared to the case in which Gr/Re = 0.

For the transverse jet, the $\psi^* = 0$ streamline indicates the upper boundary of the flow introduced by the jet. No flow ever crosses this boundary. Because the flow introduced by the jet occupies the space below this boundary, the flow originally in the channel is flowing through a smaller area, and is therefore accelerated downstream of the jet.

A positive value of Gr/Re causes the transverse jet to penetrate further into the stream than the jet for which Gr/Re = 0, particularly near the jet location. As a result of this larger "obstruction" to the flow in the channel, local regions of decelerated and accelerated flow are created near the jet (Fig. 17). A negative value of Gr/Re restricts the penetration of the jet. In this case, the flow originally in the channel is able to surpass the jet in a smooth manner (Fig. 18).

For the longitudinal jet, the effect of the buoyant force on the flow is not as pronounced as in the transverse jet. This is because the initial velocity of the jet is in the downstream direction, and therefore, the heat added by the jet is convected downstream more quickly than for the transverse jet. Hence, the local values of θ are not as great in the case of the longitudinal jet. Since the buoyant force is proportional to θ, the buoyant forces near the jet are not as great in the case of a longitudinal jet.

The effect of the buoyant force can be seen by comparing the streamlines for the case in which Gr/Re is greater than zero to the case in which Gr/Re = 0. The positive buoyant force causes the streamlines to be bent upward with respect to the case in which Gr/Re = 0 (Fig. 22). This is due to the velocity in the positive Y-direction caused by this buoyant force. A negative value of Gr/Re has the opposite effect (Fig. 23), causing the streamlines to be bent downward.

The effect of buoyancy on the temperature field for both jets can be seen by examining the isotherms presented in Figures 19–21 and 25-27. At downstream locations near the jet, temperatures are greater for a positive buoyant force than for the case in which there is no buoyant force present. This is due to the fact that a positive buoyant force contributes to the heat transfer in the vertical direction by increasing the vertical velocity component. Hence, the heat added by the jet is dispersed more quickly

in the vertical direction, and temperatures near the jet are higher. This results in an increased surface temperature. Because all heat added by the jet must leave the channel through the surface, and the amount of heat transferred at the surface is proportional to the surface temperature, more heat is transferred out of the channel near the jet for a positive buoyant force than for a zero buoyant force. Therefore the temperatures at downstream locations are lower for the positive buoyant force. This effect can be seen by examining the surface temperature data presented in Figure 30. This effect occurs for both the longitudinal and transverse jets, but is more pronounced for the transverse jet. A negative buoyant force has the opposite effect, causing the temperatures near the jet to be smaller, and the downstream temperatures higher.

V. DISCUSSION

A. CONVERGENCE OF LINEAR SOLUTION FOR STREAM FUNCTION

The validity of the matrix of linear equations for the stream function can be verified by constructing a convergence plot to determine the value to which the numerical solution would converge if an infinite number of nodes were used. This value may then be compared to an exact solution.

A convergence plot is constructed by plotting the value of the numerical solution obtained at a given point in the field of the problem versus $1/N^2$, where N is the number of divisions per side of the field. By making the number of divisions greater, different values of the numerical solution are obtained at the same point in the field. The plot of the value of the solution versus $1/N^2$ may then be extrapolated to determine the point at which the plot crosses the $1/N^2 = 0$ axis. This value of the solution is then taken as the value to which the numerical solution would converge if an infinite number of divisions were possible.

In order to apply this method to the linear (zeroth order) solution for the stream function, a fixed field must be chosen. The field chosen was a section of the channel of length 5D. The case considered was a longitudinal jet of width 2H located at the upstream boundary and in the center of the channel. By utilizing a grid in which the spacing in the X-direction is five times the spacing in the Y-direction, a grid with an equal number of divisions on

each edge of the field is possible. Convergence plots were constructed at the points $X = 2.5$, $Y = 0.25$ and $X = 2.5$, $Y = 0.75$. The mesh sizes that were used were $N = 4$, $N = 8$, and $N = 12$. The $N = 4$ grid was too coarse to yield useful convergence data. Since a grid corresponding to $N = 16$ requires excessive computer storage, only the solutions corresponding to $N = 8$ and $N = 12$ were used in the extrapolation process. The convergence plots for these two points are shown in Figures 31 and 32.

An exact solution at these two points is obtained by noting that the surface and bottom boundary conditions for the velocity are the same as those for Couette flow between flat plates. The specification of a known flow rate for incompressible flow is equivalent to specifying a driving pressure gradient in the downstream direction. Hence, for flow in the channel far enough downstream so that the effect of the jet on the flow has been damped out, the exact solution is the solution for Couette flow between flat plates with an imposed pressure gradient. This solution is given in Schlicting [14]. It should be noted that this velocity profile is parabolic in y, and that $U(0) = 0$ and $U(D) = U_S$. For an incompressible flow, the pressure gradient $\frac{\partial P}{\partial X}$ may be determined from a specified flow rate.

At the downstream boundary, several assumptions are made. It is assumed that the effect of the jet may be neglected, with the exception of the increased flow added by the jet, and that $v = 0$. It is also assumed that the velocity profile

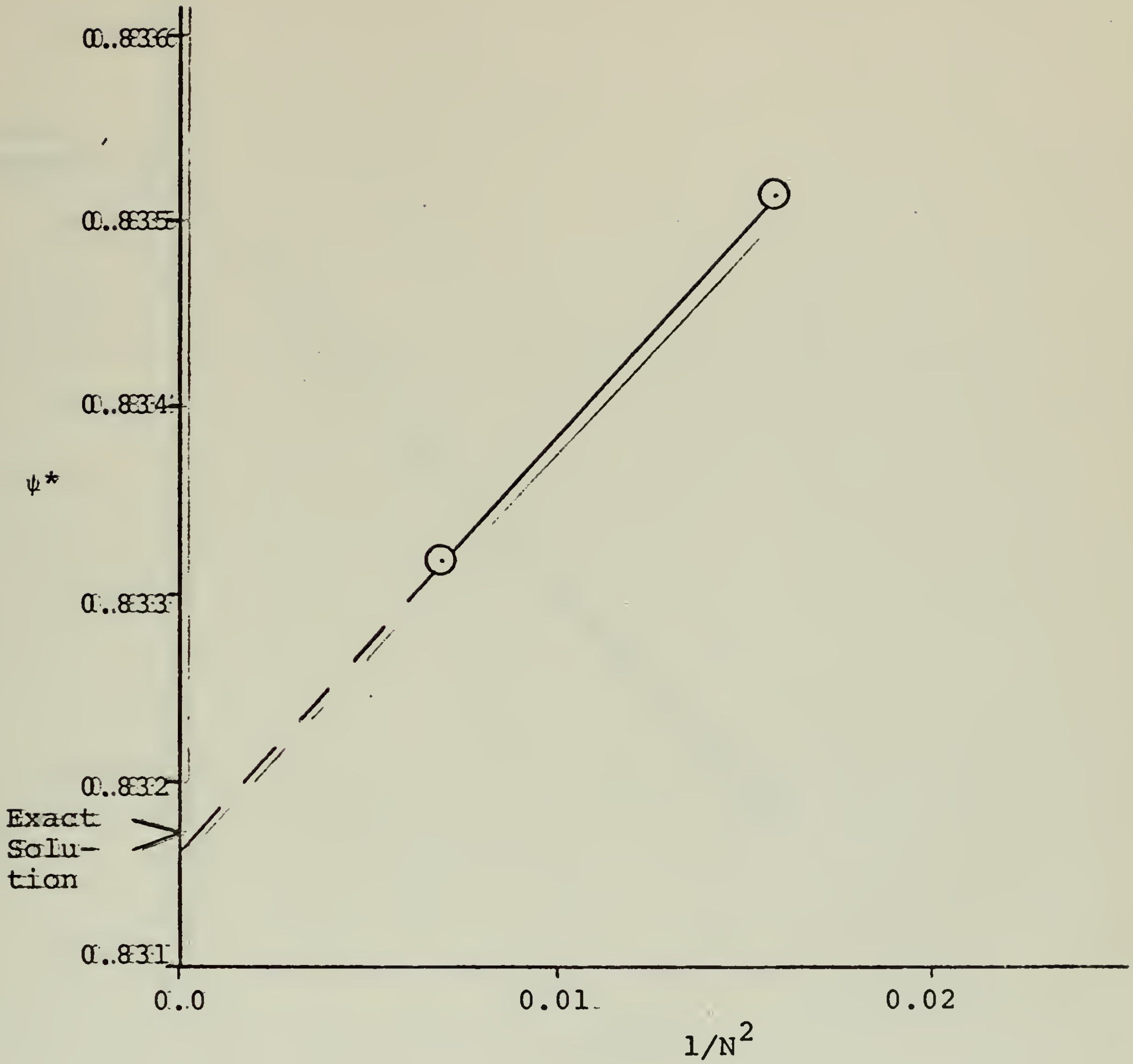

Figure 31 – Convergence plot for stream function at $X = 2.5$, $Y = 0.75$.

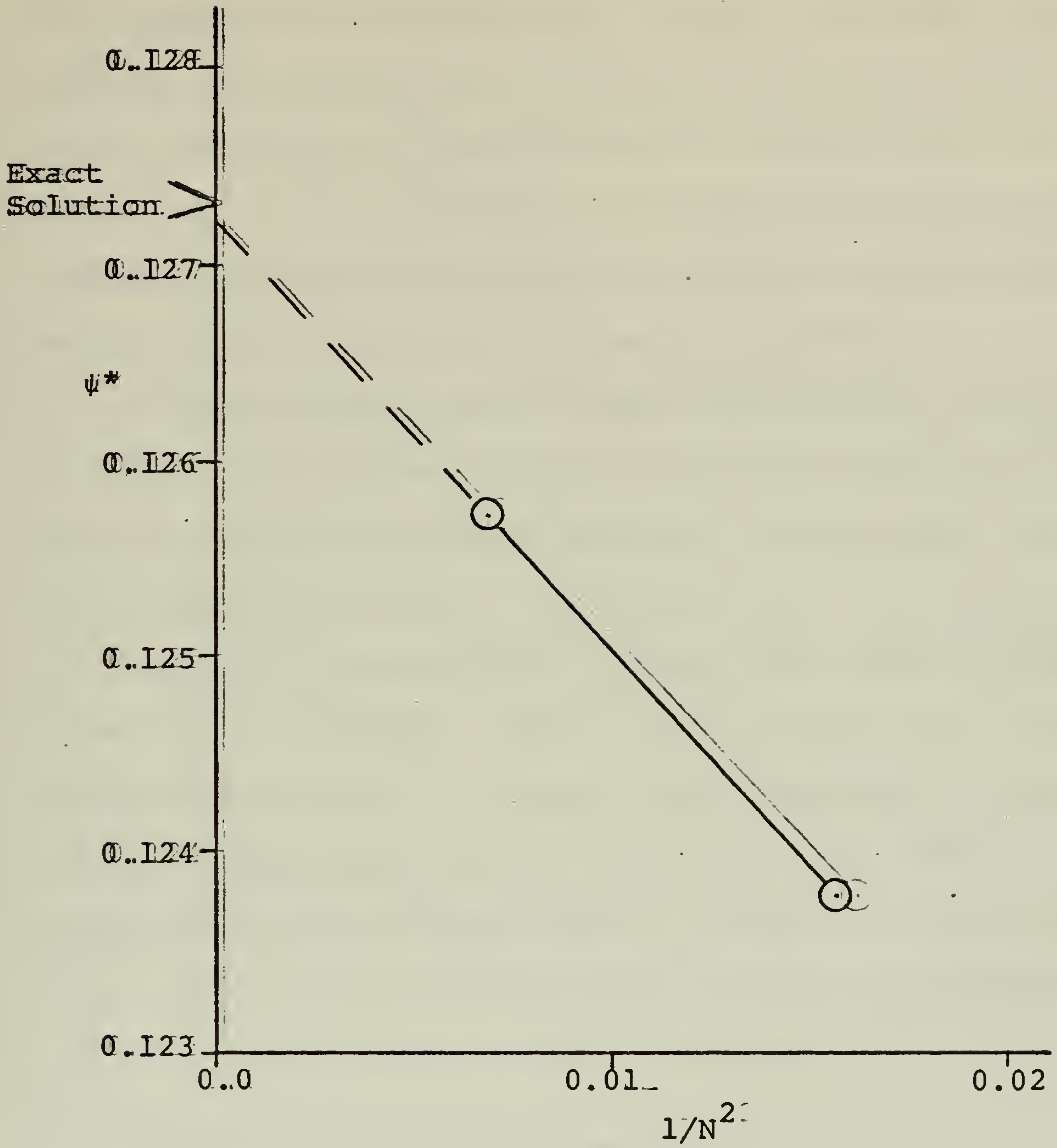

Figure 32 – Convergence plot for stream function at X = 0.25, Y = 2.5.

is parabolic in y, and that the flow rate is known. In addition, the velocity at y = 0 is equal to zero and that the velocity at y = D is equal to U_s. Since the velocity profile is parabolic in y, and since the three conditions which determine the coefficients of the parabola are identical to the conditions for Couette flow with an imposed pressure gradient, the velocity profile at the downstream boundary is identical to the exact solution.

It was assumed that the exact solution was valid at X = 2.5. The values obtained from the convergence plot may then be compared to those obtained from the exact solution. At the point X = 2.5, Y = 0.25, the exact solution is $\psi^* = 0.12723$; the solution obtained from the convergence plot is $\psi^* = 0.12731$. At the point X = 2.5, Y = 0.75, the exact solution is $\psi^* = 0.83170$; the solution obtained from the convergence plot is $\psi^* = 0.83163$. As a result of the agreement between these values, it may be concluded that the linear solution for ψ^*, which is the zeroth order solution for the iterative scheme, is valid.

B. NUMERICAL STABILITY OF ITERATIVE SCHEME

By formulating the problem in terms of the linear solutions as shown in equations (20) and (21), the nonlinear terms in the energy equation are multiplied by the Peclet number Pe, where Pe = Re Pr. The nonlinear terms in the momentum equation are multiplied by Re. However, using the iterative procedure described earlier, the numerical solution

for the energy equation becomes unstable at approximately Pe = 2. Since the energy and momentum equations are coupled, the entire solution becomes unstable at Pe = 2.

Several methods were employed in an effort to eliminate this instability. The method initially used to calculate the nonlinear terms was to use the operators shown in Figures 5, 6, and 7. Using this method, the energy equation became unstable at approximately Pe = 1. When uncoupled from the energy equation, the momentum equation became unstable at Re = 15.

The method of calculating the nonlinear terms in terms of the Jacobian as described earlier was then attempted. Using this method, the Peclet number at which instability occurred in the energy equation was raised from 1 to 2. The Reynolds number at which instability occurred in the momentum equation, uncoupled from the energy equation, was raised from 15 to 50.

Decreasing the grid spacing was also attempted. This had no noticeable effect on the stability of the system of equations.

An attempt was made to begin with the stable solution for Pe = 2.0, and increase the Peclet number in steps of 1/25. Using this procedure, instability occurred at Pe = 2.15.

C. CONCLUSIONS

Because all solutions presented in this study are based on iterations from the linear, uncoupled solutions of the derived governing equations, the validity of the numerical

methods used to obtain these solutions is of utmost importance. The validity of the operators and method of solution for the linear energy equation has been demonstrated by its frequent use with success in the literature [12, 15]. The results of the convergence plot indicate that the linear solution of the linear momentum equation is also valid. Based on these observations, it is felt that the solutions presented in this report are calculated from an essentially sound basis.

The effect of buoyancy on the flow patterns and temperature distributions has been demonstrated for the cases considered. However, the original motivation for this effort was to demonstrate the effect of buoyancy on the flow in an actual physical channel. For such channels, the actual values of Reynolds and Peclet numbers experienced are greater than 10^3. Because of the restraints on the range of Re and Pe due to nonlinear numerical instability, it was not possible to generate solutions which are applicable to actual channels.

The maximum value of the Peclet number for which results were obtained was approximately 2.0. Using the value Pr = 6 as a typical value of the Prandtl number for water, the maximum Reynolds number for which results for the coupled temperature and flow fields were obtained was approximately 0.3.

As a result of these limitations, some of the assumptions made for the boundary conditions for the longitudinal

jet may be questioned. In the formulation of the boundary condition for the temperature for the longitudinal jet, it was assumed that no heat was conducted upstream to the X-location of the jet. This assumption is valid for Pe >> 1. Since the maximum Peclet number used in the coupled problem was Pe = 1.8, this assumption is questionable.

For the velocity boundary condition for the longitudinal jet, it was assumed that the distrubance to the flow field caused by the jet does not propagate upstream to the X-location of the jet. This assumption is valid for Re >> 1. Because the maximum Reynolds number used in the solution of the coupled energy and momentum equations was 0.3, this assumption is no longer valid.

D. RECOMMENDATIONS

Using a finite difference method of solution, one algebraic equation is generated for each node. In order to solve such a system of linear algebraic equations, two basic methods exist. The first method is the direct method, which is to solve the simultaneous equations directly, generating an exact solution to the system of equations. The second method is the indirect method, which arrives at a solution by successive improvements of an approximate solution. This process is repeated until a desired convergence criteria is satisfied.

The basic method of solution used in this study was the direct method. Using this method, the number of calculations required to achieve a solution is known, which is not

true of the indirect method. The direct method is also well adapted to machine calculations. In addition, the Gaussian elimination technique of solution by the direct method is the most efficient method of solving a system of simultaneous linear algebraic equations. Using this method, however, extensive computer storage is required. For example, a finite difference solution for a grid involving 10 nodes in each direction generates 100 simultaneous equations for each unknown. In order to solve this problem by the direct method, a 100 by 100 matrix must be stored for each unknown.

On the basis of this work, the solution of nonlinear algebraic equations using the iterative method proposed earlier is not feasible when the value of the nonlinear terms becomes large. For the solution of such a problem, the indirect method of solution is recommended.

One possible method of solving such a system of nonlinear algebraic equations is to employ a numerical relaxation scheme. This method is discussed in [12]. One advantage of this method is that once the relaxation pattern is established, the need for storing matrices is eliminated.

Another possible method of solution is to recast the problem in the form of vorticity transport

$$\omega = \nabla^2 \psi^* \tag{22}$$

$$\mathrm{Re}\left[\frac{\partial \psi^*}{\partial Y}\frac{\partial \omega}{\partial X} - \frac{\partial \psi^*}{\partial X}\frac{\partial \omega}{\partial Y}\right] = \nabla^2 \omega - \frac{\mathrm{Gr}}{\mathrm{Re}}\frac{\partial \theta}{\partial Y} \tag{23}$$

$$\mathrm{Re}\,\mathrm{Pr}\left[\frac{\partial \psi^*}{\partial Y}\frac{\partial \theta}{\partial X} - \frac{\partial \psi^*}{\partial X}\frac{\partial \theta}{\partial Y}\right] = \nabla^2 \theta \tag{24}$$

where ω is the vorticity. The finite difference forms of these equations can be solved for the values of the unknown at a node in terms of the values of other unknowns at surrounding nodes. For instance, equation (22) can be solved for ω in terms of ψ^* at surrounding points. The values obtained from the previous iteration can be used to calculate new values. By choosing some appropriate starting point, an iterative solution scheme can be established.

A further recommendation is that a graded network be used in the numerical solution. This graded network should have finer divisions near the jet location. This would improve the accuracy of the method of modeling the jet, and also provide more grid points near the jet, where the maximum changes in flow and temperature are experienced.

APPENDIX A

COMPUTER PROGRAM USED TO DEVELOP FINITE DIFFERENCE OPERATORS

```
      IMPLICIT REAL*8 (A-H,O-Z)
      DIMENSION COEF(25),CM(25,25),CINV(25,25),TITLE(10),TITLE1(10),
     1 TITLE2(10),TITLE3(10),CX(25)
      READ(5,50) NUM,KSY
   50 FORMAT(2I10)
      RNUM=DFLOAT(NUM)
      SRNUM=DSQRT(RNUM)
      IDIV=SRNUM
      DO 101 JM=1,NUM
      JNDEX=(JM-1)/IDIV
      Z=DFLOAT(JNDEX)
      X=Z*KSY
      L=(JM-1-(JNDEX*IDIV))
      Y=DFLOAT(L)
      WRITE(6,60) NUM,X,Y
   60 FORMAT(7H POINT ,1I2,5X,5H X = ,1F6.1,5X,5H Y = ,1F6.2)
      CALL P(X,Y,COEF,NUM,IDIV)
      DO 100 I=1,NUM
      CM(JM,I)=COEF(I)
  100 CONTINUE
  101 CONTINUE
      WRITE(6,1)
    1 FORMAT(1H1,48X,23HMATRIX BEFORE INVERSION)
      CALL MAPRIN(25,5,CM)
      CALL INVERT(NUM,1.0D-10,CM,CINV,KER,NUM)
      IF(KER.EQ.2) WRITE(6,1000)
 1000 FORMAT(//,19H MATRIX IS SINGULAR,//)
      WRITE(6,2)
    2 FORMAT(1H1,48X,22HMATRIX AFTER INVERSION)
      CALL MAPRIN(25,5,CINV)
      DO 200 I=1,NUM
  200 CX(I)=0.0D0
  300 READ(5,350) IDX,IDY,KODE,CMUL
  350 FORMAT(3I10,1F10.0)
      WRITE(6,20) IDX,IDY
   20 FORMAT(1H1,15X,5HIDX =,1I3,5X,5HIDY =,1I3)
      YVALU=2.0D0*KSY
      CALL DP(YVALU,2.0D0,IDX,IDY,COEF,NUM,IDIV)
      DO 400 I=1,NUM
      COEF(I)=CMUL*COEF(I)
      CX(I)=CX(I)+COEF(I)
      WRITE(6,21) COEF(I),CX(I)
   21 FORMAT(1H0,2D20.10)
  400 CONTINUE
      IF(KODE.EQ.0) GO TO 300
      DO 800 I=1,25
      COEF(I)=0.0D0
      DO 800 J=1,25
```

```
      COEF(I)=COEF(I)+(CX(J)*CINV(J,I))
  800 CONTINUE
      DO 801 I=1,25
      CC=COEF(I)
      CC=DABS(CC)
  801 IF(CC.LT.1.0D-10) COEF(I)=0.0D0
      WRITE(6,3)
    3 FORMAT(1H1,2X,21HDIFFERENTIAL OPERATOR)
      DO 1100 I=1,NUM
      WRITE(6,1050) I,COEF(I)
 1050 FORMAT(1H0,10X,1I6,3X,1D20.10)
 1100 CONTINUE
      WRITE(6,1060)
 1060 FORMAT(1H1,25HOPERATOR MULTIPLIED BY 72)
      DO 1055 I=1,NUM
      COEF(I)=72.0D0*COEF(I)
      WRITE(6,1050) I,COEF(I)
 1055 CONTINUE
      STOP
      END


      SUBROUTINE MAPRIN(NUM,IDIV,A)
      IMPLICIT REAL*8 (A-H,O-Z)
      DIMENSION A(NUM,NUM)
      DO 200 I=1,IDIV
      I1=1+5*(I-1)
      I2=2+5*(I-1)
      I3=3+5*(I-1)
      I4=4+5*(I-1)
      I5=5+5*(I-1)
      WRITE(6,100) I1,I2,I3,I4,I5
  100 FORMAT(1H0,10X,3HROW,1I3,18X,3HROW,1I3,18X,3HROW,1I3,18X,3HROW,1I3
     C,18X,3HROW,1I3)
      DO 200 J=1,NUM
      WRITE(6,120) J,A(I1,J),J,A(I2,J),J,A(I3,J),J,A(I4,J),J,A(I5,J)
  120 FORMAT(1I3,1D20.10,1I3,1D20.10,1I3,1D20.10,1I3,1D20.10,1I3,1D20.10
     ")
  200 CONTINUE
      RETURN
      END


       SUBROUTINE INVERT(N,EP,A,X,KER,NACT)
      IMPLICIT REAL*8 (A-H,O-Z)
      DIMENSION A(NACT,NACT),X(NACT,NACT)
      DO 1 I=1,N
      DO 1 J=1,N
```

```
  1 X(I,J)=0.0D0
    DO 2 K=1,N
  2 X(K,K)=1.0D0
 10 DO 34 L=1,N
    KP=0
    Z=0.0D0
    DO 12 K=L,N
    IF(Z-DABS(A(K,L)))11,12,12
 11 Z=DABS(A(K,L))
    KP=K
 12 CONTINUE
    IF(L-KP)13,20,20
 13 DO 14 J=L,N
    Z=A(L,J)
    A(L,J)=A(KP,J)
 14 A(KP,J)=Z
    DO 15 J=1,N
    Z=X(L,J)
    X(L,J)=X(KP,J)
 15 X(KP,J)=Z
 20 IF(DABS(A(L,L))-EP)50,50,30
 30 IF(L-N)31,34,34
 31 LP1=L+1
    DO 36 K=LP1,N
    IF(A(K,L))32,36,32
 32 RATIO=A(K,L)/A(L,L)
    DO 33 J=LP1,N
 33 A(K,J)=A(K,J)-RATIO*A(L,J)
    DO 35 J=1,N
 35 X(K,J)=X(K,J)-RATIO*X(L,J)
 36 CONTINUE
 34 CONTINUE
 40 DO 43 I=1,N
    II=N+1-I
    DO 43 J=1,N
    S=0.0D0
    IF(II-N)41,43,43
 41 IIP1=II+1
    DO 42 K=IIP1,N
 42 S=S+A(II,K)*X(K,J)
 43 X(II,J)=(X(II,J)-S)/A(II,II)
    KER=1
    GO TO 75
 50 KER=2
 75 CONTINUE
    RETURN
    END
```

```
      SUBROUTINE DP(X,Y,IDX,IDY,COEF,NUM,IDIV)
      IMPLICIT REAL*8 (A-H,O-Z)
      DIMENSION COEF(25)
      DO 100 I=1,NUM
      INDEX=(I-1)/IDIV
      IXX=IDIV-1-INDEX
      IYY=IDIV-I+(INDEX*IDIV)
      IF(IDX.GT.IXX) GO TO 50
      IF(IDY.GT.IYY) GO TO 50
      KKX=1
      IF(IDX.EQ.0) GO TO 20
      DO 10 K=1,IDX
      KN=IXX-K+1
      KKX=KKX*KN
   10 CONTINUE
   20 CONTINUE
      KKY=1
      IF(IDY.EQ.0) GO TO 40
      DO 30 J=1,IDY
      KNY=IYY-J+1
      KKY=KKY*KNY
   30 CONTINUE
   40 CONTINUE
      KK=KKX*KKY
      CK=DFLOAT(KK)
      IXX=IXX-IDX
      IYY=IYY-IDY
      IF(IXX.EQ.0) GO TO 90
      IF(IYY.EQ.0) GO TO 95
      COEF(I)=(X**IXX)*(Y**IYY)*CK
      GO TO 99
   90 CONTINUE
      IF(IYY.EQ.0) GO TO 91
      COEF(I)=(Y**IYY)*CK
      GO TO 99
   91 COEF(I)=CK
      GO TO 99
   50 COEF(I)=0.0D0
      GO TO 99
   95 COEF(I)=(X**IXX)*CK
   99 CONTINUE
  100 CONTINUE
      RETURN
      END
```

```
      SUBROUTINE P(X,Y,COEF,NUM,IDIV)
      IMPLICIT REAL*8 (A-H,O-Z)
      DIMENSICN COEF(NUM)
      DO 100 I=1,NUM
      INDEX=(I-1)/IDIV
      IXX=IDIV-1-INDEX
      IYY=IDIV-I+(INDEX*IDIV)
      IF(IXX.EQ.0) GO TO 90
      IF(IYY.EQ.0) GO TO 95
      COEF(I)=(X**IXX)*(Y**IYY)
      GO TO 99
   90 CONTINUE
      IF(IYY.EQ.0) GO TO 91
      COEF(I)=Y**IYY
      GO TO 99
   91 COEF(I)=1.0D0
      GO TO 99
   95 COEF(I)=X**IXX
   99 CONTINUE
  100 CONTINUE
      RETURN
      END
```

APPENDIX B

COMPUTER PROGRAM USED IN NUMERICAL SOLUTION

```
// EXEC FORTCLG,REGION,GO=250K
//FORT.SYSIN DD *
      IMPLICIT REAL*8 (A-H,O-Z)
      DIMENSION KODE(133),SI(133),T(133),KKOD(133)
      DIMENSION CTI(119,119),TK(119),TKI(119),TK1(119),TKF(119)
      DIMENSION CSI(85,85),CK(85),CKI(85),CK1(85),DEL(85),
     "CSI1(25),CSI2(25),COEF(25),CTF(9),DY5(5),DX5(5),INT(9)
      DO 52 I=1,5
      J1=(I-1)*5+1
      J2=I*5
      READ(5,51)(COEF(J),J=J1,J2)
   51 FORMAT(5F10.0)
   52 CONTINUE
      READ(5,55)(CTF(J),J=1,9)
   55 FORMAT(9F8.4)
      READ(5,56) N,M
   56 FORMAT(2I10)
      READ(5,57) UJ,DJ,Q,BI,TA
   57 FORMAT(5F10.5)
      READ(5,58) IJ1,IJ2,UX,UY,XMUL
   58 FORMAT(2I10,3F10.4)
C     N=# OF NODES IN X-DIRECTION,M=# OF NODES IN Y-DIRECTION
      US=9.0D0/7.0D0
      NQQ=0
      NQ1=0
      NQ2=0
      NUM=N*M
      NUP=NUM-(2*M)
      DO 210 I=1,NUP
      DO 210 J=1,NUP
      TK(I)=0.0D0
  210 CTI(I,J)=0.0D0
      DO 5 I=1,NUM
      T(I)=0.0D0
    5 SI(I)=0.0D0
      DO 59 I=1,N
      J=M*I
      SI(J)=1.0D0
      K=M*(I-1)+1
   59 IF(K.GT.IJ2) SI(K)=-UJ*DJ
      RM=DFLOAT(M-1)
      H=1.0D0/RM
C     KODE=1 AT KNOWN VALUES OF PSI
      DO 1 I=1,NUM
    1 KODE(I)=0
      DO 2 I=1,M
      J=I+(N-1)*M
      KODE(I)=1
```

```
    2 KODE(J)=1
      DO 3  I=2,N
      J=1+(I-1)*M
      K=J+M-1
      KODE(J)=1
    3 KODE(K)=1
      N1=NUM-M+1
      DO 4  I=N1,NUM
    4 KODE(I)=1
C     SI(I) ARE KNOWN VALUES OF PSI
      DO 10 I=1,M
      Y=(I-1)*H
      SI(I)=(12.0D0*(Y**2)-5.0D0*(Y**3))/7.0D0
      IF(I.EQ.IJ2) SI(I)=SI(I)+UJ*DJ/2.0D0
      IF(I.GT.IJ2) SI(I)=SI(I)+UJ*DJ
      J=I+(N-1)*M
      SI(J)=((12.0D0/7.0D0+3.0D0*UJ*DJ)*(Y**2)-(5.0D0/7.0D0+2.0D0*UJ*DJ)
     C*(Y**3))-UJ*DJ
      T(I)=0.0D0
   10 T(J)=0.0D0
C     CSI(I,J)=COEFFICIENTS IN MATRIX OF PSI UNKNOWNS
      NUN=(M-2)*(N-2)
      DO 60 I=1,NUN
      DO 60 J=1,NUN
   60 CSI(I,J)=0.0D0
      DO 61 I=1,NUP
   61 TKF(I)=0.0D0
      MM2=M-2
      DSI1=-UY*H
      DSI2=UX*H
      DO 70 I=1,MM2
      IP1=I+1
      IK=IP1+2.0D0*M
      J=I+M-2
           CSI(I,I)=4.0D0
      CSI(I,J)=-1.0D0
      CK(I)=SI(IP1)*3.0D0
   70 CONTINUE
      NM2=N-2
      NIT=0
      DO 200 NCOL=3,NM2
      J1=(NCOL-2)*(M-2)
      I2=1+(NCOL-1)*M
      J2=J1+1
      J3=J1+2
      IK=I2+2
      CSI(J2,J2)=4.0D0
      CSI(J2,J3)=-1.0D0
```

```
      CK(J2)=3.0D0*SI(I2)
      K1=3+(NCOL-1)*M
      K2=(M-2)+(NCOL-1)*M
      DO 190 K=K1,K2
      J2=J2+1
      CK(J2)=0.0D0
      L=0
      DO 120 KK=1,5
      KKK=KK-3
      DO 120 II=1,5
      L=L+1
      INDI=K+KKK*M+II-3
      KOD=KODE(INDI)
      IF(KOD.EQ.1) GO TO 99
      INDJ=J2+KKK*(M-2)+II-3
      CSI(J2,INDJ)=COEF(L)
      GO TO 120
   99 CONTINUE
      CK(J2)=CK(J2)-COEF(L)*SI(INDI)
  120 CONTINUE
  190 CONTINUE
      I=NCOL*M
      J=(NCOL-1)*(M-2)
      I1=I-1
      J1=J-1
      IK=I-2
      CSI(J,J)=-4.0D0
      CSI(J,J1)=1.0D0
      CK(J)=-3.0D0*SI(I)+2.0D0*H*US
  200 CONTINUE
      TJ=1.0D0
      T(IJ2)=TJ
      DO 201 II=1,MM2
      I=(N-1)*M+II+1
      J=(N-3)*(M-2)+II
      JM1=J-(M-2)
      CSI(J,J)=-4.0D0
      CSI(J,JM1)=1.0D0
      IK=I-2.0D0*M
      CK(J)=(-3.0D0)*SI(I)
  201 CONTINUE
      NM1=N-1
      JJZ=IJ2+M
      T(JJZ)=1.0D0
      DO 300 NCOL=2,NM1
      N1=M*(NCOL-2)+1
      N2=M*(NCOL-2)+2
      N3=M*(NCOL-2)+3
```

```
      I3=N3+M
      IF(I3.EQ.IJ2) TK(N1)=1.0D0*TJ
      CTI(N1,N1)=-3.0D0
      CTI(N1,N2)=4.0D0
      CTI(N1,N3)=-1.0D0
      MM1=M-1
      DO 220 KM=2,MM1
      I=(NCOL-1)*M+KM
      J=(NCOL-2)*M+KM
      L=0
      DO 220 KK=1,3
      KKK=KK-2
      DO 220 II=1,3
      L=L+1
      INTI=I+KKK*M+II-2
      IF(INTI.EQ.JJ2) GO TO 214
      IF(INTI.EQ.IJ2) GO TO 214
      NCR=NUM-M
      IF(INTI.LE.M) GO TO 215
      IF(INTI.GT.NCR) GO TO 215
      INTJ=J+KKK*M+II-2
      CTI(J,INTJ)=CTF(L)
      GO TO 215
  214 TK(J)=-CTF(L)*T(INTI)
  215 CONTINUE
  220 CONTINUE
      N1=(NCOL-1)*M
      N2=(NCOL-1)*M-1
      N3=(NCOL-1)*M-2
      I3=N3+M
      TK(N1)=2.0D0*H*BI*(Q-TA)*(-1.0D0)
      I2=N2+M
      CTI(N1,N1)=3.0D0+2.0D0*H*BI
      CTI(N1,N2)=-4.0D0
      CTI(N1,N3)=1.0D0
      IF(I3.EQ.IJ2) TK(N1)=TK(N1)-TJ
      IF(I2.EQ.IJ2) TK(N1)=4.0D0*TJ+TK(N1)
  300 CONTINUE
      J2=IJ2-M
      DO 301 I=1,NUP
      CTI(I,J2)=0.0D0
      CTI(IJ2,I)=0.0D0
      CTI(I,IJ2)=0.0D0
  301 CTI(J2,I)=0.0D0
      CTI(IJ2,IJ2)=1.0D0
      CTI(J2,J2)=1.0D0
      TK(J2)=1.0D0
      JQ=IJ2-M+1
```

```
      TK(JQ)=-1.0D0
      TK(IJ2)=1.0D0
      JJ=IJ2+M
      T(JJ)=1.0D0
      T(IJ2)=1.0D0
      NNN=0
      DO 705 I=1,5
      J1=(I-1)*5+1
      J2=I*5
      READ(5,701) (CSI1(J),J=J1,J2)
701   FORMAT(5F10.4)
705   CONTINUE
      DO 710 I=1,5
      J1=(I-1)*5+1
      J2=I*5
      READ(5,706)(CSI2(J),J=J1,J2)
706   FORMAT(5F10.4)
710   CONTINUE
      READ(5,711)(DY5(I),I=1,5)
      READ(5,711)(DX5(I),I=1,5)
711   FORMAT(5F10.4)
      READ(5,645) GRDRE,RE,PR
645   FORMAT(3F10.3)
      DO 660 I=1,NUN
660   CKI(I)=CK(I)
      DO 661 I=1,NUP
661   TKI(I)=TK(I)
      DO 819 I=1,NUP
819   TK1(I)=0.0D0
      CALL ELU(CTI,NUP,NUP)
      CALL ELU(CSI,NUN;NUN)
709   NNN=NNN+1
      DO 872 I=1,NUP
872   TKF(I)=TK(I)
712   CONTINUE
      NIT=0
611   CONTINUE
      ITOL=0
      NIT=NIT+1
      NUN=(N-2)*(M-2)
      CALL SOLVB(CSI,NUN,NUN,CK)
      IF(NIT.EQ.1) GO TO 605
      DO 603 I=1,NUN
      TOL=(CK(I)-CK1(I))/CK(I)
      TOL=DABS(TOL)
      IF(TOL.GT.0.0001D0) ITOL=1
603   CONTINUE
605   CONTINUE
```

```
      DO 669 I=1,NUN
      IF(NNN.EQ.1.AND.NIT.EQ.1) GO TO 669
      CKK=CK(I)
      SIK=1.0D0+UJ*DJ
      SIM=-UJ*DJ
      IF(CKK.LT.SIM) CK(I)=1.01D0*CK1(I)
      IF(CKK.GT.SIK) CK(I)=0.9D0*CK1(I)
  669 CONTINUE
      DO 670 NCOL=2,NM1
      NM1=N-1
      MM1=M-1
      DO 670 K=2,MM1
      I=(NCOL-1)*M+K
       J=(NCOL-2)*(M-2)+K-1
  670 SI(I)=CK(J)
      DO 604 I=1,NUN
  604 CK1(I)=CK(I)
      DO 613 I=1,NUP
  613 TK(I)=TKI(I)
      IF(NIT.EQ.1) ITOL=1
      GO TO 686
  664 CONTINUE
      WRITE(6,681) NIT
  681 FORMAT(1H1,15X,12HITERATION NO,1I6)
      WRITE(6,683) UX,UY
  683 FORMAT(1H0,10X,4HUX =,1F8.1,5X,4HUY =,1F8.1)
      WRITE(6,682) RE,PR,GRDRE
  682 FORMAT(1H0,10X,4HRE =,1F8.4,5X,4HPR =,1F8.1,5X,7HGR/RE =,1F8.1)
      WRITE(6,665)
  665 FORMAT(1H0,25X,15HSTREAM FUNCTION)
      DO 685 I=1,NUM
      WRITE(6,680) I,SI(I)
  680 FORMAT(10X,5HPOINT,1I6,5X,1D13.6,10X,1D13.6)
  685 CONTINUE
  686 CONTINUE
  614 CONTINUE
      DO 713 I=1,NUM
  713 KKOD(I)=0
      NM2=N-2
      MM2=M-2
      DO 714 NCOL=3,NM2
      DO 714 K=3,MM2
      I=(NCOL-1)*M+K
  714 KKOD(I)=1
      MM1=M-1
      NM1=N-1
  653 CONTINUE
      DO 15 I=1,NUN
```

```
 15 DEL(I)=0.0
    DO 50 NCOL=2,NM1
     DO 50 K=2,MM1
    I=(NCOL-1)*M+K
    J=(NCOL-2)*(MM2)+K-1
    L=0
    DO 20 KK=1,3
    KKK=KK-2
    DO 20 II=1,3
    L=L+1
    INTI=I+KKK*M+II-2
    DEL(J)=DEL(J)+CTF(L)*SI(INTI)
 20 CONTINUE
 50 CONTINUE
    DO 612 I=1,NUN
    CK(I)=CKI(I)
612 CONTINUE
    DO 920 NCOL=3,NM2
    DO 920 K=3,MM2
    I=(NCOL-1)*M+K
    J=(NCOL-2)*MM2+K-1
    CALL OPER(I,M,I1,I2,I3,I4,I5,I6,I7,I8,I9)
    CALL OPER(J,MM2,J1,J2,J3,J4,J5,J6,J7,J8,J9)
    RJPP=(SI(I8)-SI(I2))*(DEL(J6)-DEL(J4))-(SI(I6)-SI(I4))*(DEL(J8)-DE
   CL(J2))
    RJCP=SI(I8)*(DEL(J9)-DEL(J7))-SI(I2)*(DEL(J3)-DEL(J1))-SI(I6)*(DEL
   C(J9)-DEL(J3))+SI(I4)*(DEL(J7)-DEL(J1))
    RJPC=DEL(J6)*(SI(I9)-SI(I3))-DEL(J4)*(SI(I7)-SI(I1))-DEL(J8)*(SI(I
   C9)-SI(I7))+DEL(J2)*(SI(I3)-SI(I1))
    TT=(RJPP+RJPC+RJCP)*6.0D0/XMUL
    CK(J)=CKI(J)-TT*RE
920 CONTINUE
    NM2=N-2
    MM2=M-2
    DO 650 NCOL=3,NM2
    DO 650 K=3,MM2
    I=(NCOL-1)*M+K
    IF(I.EQ.IJ2)GO TO 650
    J=(NCOL-2)*(M-2)+K-1
    I1=I-M
    I2=I+M
    CK(J)=CK(J)-0.5D0*(T(I1)-T(I2))*(GRDRE)*72.0D0*(H**3)/XMUL
650 CONTINUE
    IF(ITOL.EQ.0) GO TO 800
    GO TO 611
800 CONTINUE
817 CONTINUE
    NOK=0
```

```
818 CONTINUE
    DO 875 I=1,NUP
875 TK(I)=TKI(I)
    NOK=NOK+1
    IF(NNN.EQ.1.AND.NOK.EQ.1)GO TO 836
    DO 720 NCOL=2,NM1
    DO 720 K=2,MM1
    I=(NCOL-1)*M+K
    J=I-M
    CALL OPER(I,M,I1,I2,I3,I4,I5,I6,I7,I8,I9)
    TPP=(SI(I8)-SI(I2))*(T(I6)-T(I4))-(SI(I6)-SI(I4))*(T(I8)-T(I2))
    TPC=SI(I8)*(T(I9)-T(I7))-SI(I2)*(T(I3)-T(I1))-SI(I6)*(T(I9)-T(I3))
   "+SI(I4)*(T(I7)-T(I1))
    TCP=T(I6)*(SI(I9)-SI(I3))-T(I4)*(SI(I7)-SI(I1))-T(I8)*(SI(I9)-SI(I
   C7))+T(I2)*(SI(I3)-SI(I1))
    TT=(TPP+TCP+TPC)*RE*PR/(12.0D0*XMUL)
    TK(J)=TKI(J)-TT
720 CONTINUE
836 CONTINUE
    J2=IJ2-M
    TK(IJ2)=1.0D0
    TK(J2)=1.0D0
    CALL SOLVB(CTI,NUP,NUP,TK)
    ITT=0
    DO 850 I=1,NUP
    TTL=(TK(I)-TK1(I))/TK(I)
    TTL=DABS(TTL)
    IF(TTL.GT.0.0001D0) ITT=1
    TKK1=TK1(I)
    TKK=TK(I)
    IF(TKK1.EQ.0.0D0) GO TO 906
    IF(TKK.LT.0.0D0) TK(I)=TK1(I)*1.01D0
    IF(TKK.GT.1.0D0) TK(I)=0.9*TK1(I)
906 CONTINUE
850 CONTINUE
    DO 851 I=1,NUP
851 TK1(I)=TK(I)
    NM1=N-1
    DO 620 NCOL=2,NM1
    DO 620 K=1,M
    I=(NCOL-1)*M+K
    J=(NCOL-2)*M+K
620 T(I)=TK(J)
    IF(ITT.EQ.1) GO TO 818
    WRITE(6,853) NOK
853 FORMAT(1H1,10X,13H TEMP ITER NO,2I6)
    WRITE(6,682) RE,PR,GRDRE
    WRITE(6,852)
```

```
852  FORMAT(1H0,25X,15HSTREAM FUNCTION,10X,11HTEMPERATURE)
     DO 854 I=1,NUM
854  WRITE(6,680) I,SI(I),T(I)
     IFT=0
     IF(NNN.EQ.1) GO TO 709
     DO 870 I=1,NUP
     FTOL=(TKF(I)-TK(I))/TK(I)
     FTOL=DABS(FTOL)
     IF(FTOL.GT.0.0001) IFT=1
870  CONTINUE
     IF(IFT.EQ.1) GO TO 709
     WRITE(6,871)
871  FORMAT(1H0,40X,23H SOLUTION HAS CONVERGED)
     READ(5,1002) GRDRE,RE,PR,III
1002 FORMAT(3F10.5,1I10)
     IF(III.EQ.1) GO TO 712
     STOP
     END


     SUBROUTINE ELU(A,N,ND)
     IMPLICIT REAL*8 (A-H,O-Z)
     DIMENSION A(ND,ND)
     NM1=N-1
     DO 100 K=1,NM1
     KP1=K+1
     DO 100 I=KP1,N
     G=-A(I,K)/A(K,K)
     A(I,K)=G
     DO 100 J=KP1,N
100  A(I,J)=A(I,J)+G*A(K,J)
     RETURN
     END


     SUBROUTINE SOLVB(A,N,ND,B)
     IMPLICIT REAL*8 (A-H,O-Z)
     DIMENSION A(ND,ND),B(ND)
     NM1=N-1
     NP1=N+1
     DO 100 K=1,NM1
     KP1=K+1
     DO 100 I=KP1,N
100  B(I)=B(I)+A(I,K)*B(K)
     B(N)=B(N)/A(N,N)
     DO 300 K=2,N
     I=NP1-K
     J1=I+1
```

```
      DO 200 J=J1,N
  200 B(I)=B(I)-A(I,J)*B(J)
  300 B(I)=B(I)/A(I,I)
      RETURN
      END

      SUBROUTINE OPER(I,M,I1,I2,I3,I4,I5,I6,I7,I8,I9)
      I1=I-M-1
      I2=I1+1
      I3=I1+2
      I4=I-1
      I5=I
      I6=I+1
      I7=I+M-1
      I8=I7+1
      I9=I7+2
      RETURN
      END
```

LIST OF REFERENCES

1. European Inland Fisheries Advisory Commission Working Party on Water Quality Criteria for European Freshwater Fish, "Water Quality Criteria for European Freshwater Fish — Water Temperature and Inland Fisheries," Water Research, v. 3, pp. 641-652, 1969.

2. Sefchovich, E., "The Preliminary Thermal Analysis of a Body of Water in Power Plant Siting," Environmental Effects of Thermal Discharges, presented at Winter Annual Meeting of the American Society of Mechanical Engineers, 1970, pp. 19-25, American Society of Mechanical Engineers, 1970.

3. Nahavandi, A. N. and Campisi, J., "A Parametric Study on the Thermal Pollution of Rivers by Stream Power Plants," Environmental Effects of Thermal Discharges, presented at Winter Annual Meeting of the American Society of Mechanical Engineers, 1970, pp. 26-34, American Society of Mechanical Engineers, 1970.

4. Merriam, Daniel, "The Calefaction of a River," Scientific American, v. 222, n. 5, pp. 42-61, 1970.

5. Polk, Edward M., Benedict, Barry A., and Parker, Frank L., "Dispersion of Thermal Discharges in Bodies of Water," Heat Transfer Aspects of Commercial Power Generation, pp. 111-119, American Institute of Chemical Engineers, 1971.

6. Brand, R. S. and Lahey, F. J., "The Heated Laminar Vertical Jet," Journal of Fluid Mechanics, v. 29, pp. 305-315, 1967.

7. Wiley, J., Personal Communication, Mechanical Engineering Department, Oregon State University, 1972.

8. Ramsey, J. W. and Goldstein, R. J., "Interaction of a Heated Jet with a Deflecting Stream," Journal of Heat Transfer, v. 93, n. 4, pp. 365-372.

9. Tulin, Marshall P. and Schwartz, Josef, "Hydrodynamic Aspects of Waste Discharge," Journal of Hydronautics, v. 6, n. 1, 1972.

10. Linsley, Ray K., Jr., Kohler, Max. A. and Paulhus, Joseph L. H., Hydrology for Engineers, p. 61, McGraw-Hill, 1958.

11. Dias, Gerald Frietas, An Investigation of a New Class of Finite Difference Operators to be Used in Solution of Partial Differential Equations, M. S. Thesis, Naval Postgraduate School, 1970.

12. Crandall, Stephen H., Engineering Analysis, pp. 246-251, McGraw-Hill, 1956.

13. Haltmer, G. J., Numerical Weather Prediction, pp. 208, 209, Wiley, 1971.

14. Schlicting, Hermann, Boundary Layer Theory, p. 77, McGraw-Hill, 1968.

15. Salvadori, Mario G. and Baron, Melvin L., Numerical Methods in Engineering, pp. 206-209, Prentice-Hall, 1961.

INITIAL DISTRIBUTION LIST

		No. Copies
1.	Defense Documentation Center Cameron Station Alexandria, Virginia 22314	2
2.	Library, Code 0212 Naval Postgraduate School Monterey, California 93940	2
3.	Mechanical Engineering Department, Code 59 Naval Postgraduate School Monterey, California 93940	1
4.	Asst. Professor M. D. Kelleher, Code 59Kk Naval Postgraduate School Monterey, California 93940	2
5.	ENS Gerald Champagne 2740 Ransford Avenue, Apt. 3 Pacific Grove, California 93950	1

DOCUMENT CONTROL DATA - R & D

(Security classification of title, body of abstract and indexing annotation must be entered when the overall report is classified)

1. ORIGINATING ACTIVITY *(Corporate author)* Naval Postgraduate School Monterey, California 93940	2a. REPORT SECURITY CLASSIFICATION Unclassified 2b. GROUP

3. REPORT TITLE

Analysis of a Heated Jet in a Stream

4. DESCRIPTIVE NOTES *(Type of report and, inclusive dates)*

Master's Thesis; June 1972

5. AUTHOR(S) *(First name, middle initial, last name)*

Gerald Edward Champagne

6. REPORT DATE June 1972	7a. TOTAL NO. OF PAGES 98	7b. NO. OF REFS 15

8a. CONTRACT OR GRANT NO.	9a. ORIGINATOR'S REPORT NUMBER(S)
b. PROJECT NO.	
c.	9b. OTHER REPORT NO(S) *(Any other numbers that may be assigned this report)*
d.	

10. DISTRIBUTION STATEMENT

Approved for public release; distribution unlimited.

11. SUPPLEMENTARY NOTES	12. SPONSORING MILITARY ACTIVITY Naval Postgraduate School Monterey, California 93940

13. ABSTRACT

A plane, heated jet of a constant property fluid exiting into a plane, straight channel of the same fluid is analyzed. The effect of buoyancy on the velocity and temperature fields is investigated. Two jet orientations are considered; a transverse jet, which enters the stream perpendicular to the main flow, and a longitudinal jet, which enters the stream parallel to the main flow.

Solutions for the temperature and velocity fields for low Reynolds number flow are obtained using a finite difference scheme. Results are presented for three different values of the buoyant force, holding other variables constant. For an isothermal jet, results for the velocity field are presented at a higher Reynolds number.

Security Classification

KEY WORDS	LINK A		LINK B		LINK C	
	ROLE	WT	ROLE	WT	ROLE	WT
Heated Jet						
Buoyant Jet						

FORM 1 NOV 65 1473 (BACK)
0101-507-6821

Security Classification

A-31409

Thesis 134829
C35 Champagne
c.1 Analysis of a heated
jet in a stream.